



**UNIVERSITY OF ZIMBABWE**

**FACULTY OF ENGINEERING**

**DEPARTMENT OF CIVIL ENGINEERING**



A remote sensing based approach to determine  
evapotranspiration in the Mbire District of Zimbabwe

**Hubert Samboko**

MSc. Thesis in WREM

**HARARE, JUNE 2016**

**UNIVERSITY OF ZIMBABWE**

**FACULTY OF ENGINEERING**

**DEPARTMENT OF CIVIL ENGINEERING**



**A remote sensing based approach to determine evapotranspiration in the  
Mbire District of Zimbabwe**

**By**

**Hubert Samboko**

**Supervisors**

**Mr. Webster GUMINDOGA**

**Dr. Eng. Hodson MAKURIRA**

**A thesis submitted in partial fulfillment of the requirements for the degree of Master of Science  
in Water Resources Engineering and Management of the University of Zimbabwe**

**JUNE 2016**

## **DECLARATION**

**I, Hubert Samboko**, assert that this thesis report is my work. It is being submitted for a degree in a Master of Science in Water Resources Engineering and Management (WREM) of the University of Zimbabwe. It has not been submitted before for assessment in any other University for any degree

**Date:** \_\_\_\_\_

**Signature:** \_\_\_\_\_

## **Disclaimer**

This document presents work that has been undertaken as part of the programme of study at the University of Zimbabwe, Civil Engineering Department. All views and opinions expressed therein remain the sole responsibility of the author, and do not automatically represent those of the institution (University of Zimbabwe).

## Table of Contents

DECLARATION.....	i
Disclaimer.....	ii
List of Tables.....	v
List of Figures.....	vi
Dedication.....	viii
Acknowledgements.....	ix
ABSTRACT.....	x
1. INTRODUCTION.....	11
1.1 Background.....	11
1.2 Problem Statement.....	13
1.3 Justification.....	14
1.4 Hypothesis.....	14
1.5 Main Objective.....	15
1.5.1 Specific Objectives.....	15
1.6 Thesis structure.....	15
2. LITERATURE REVIEW.....	16
2.1 Water balance of semi-arid areas.....	16
2.2 Evapotranspiration.....	16
2.2.1 Estimation of evapotranspiration.....	16
2.2.2 Methods of estimating potential evapotranspiration.....	16
2.2.3 Remote Sensing approaches in estimating evapotranspiration.....	18
2.3 Surface Energy Balance System algorithm theory.....	22
2.3.1 Roughness.....	24
2.3.2 Advection-aridity evapotranspiration method.....	25
2.4 Hydrological modeling techniques for water balance assessments.....	26
2.4.1 HEC-HMS.....	27
2.4.2 HBV Model.....	29
2.4.3 The Curve Number method.....	30
2.4.4 The TOPMODEL Concept.....	31
2.5 Determination of water availability and consumption.....	32
2 MATERIALS AND METHODS.....	33
3.1 Description of study area.....	33
3.1.1 Climate.....	34
3.1.2 Soils and Geology.....	35
3.1.3 Livelihoods and Socio-economic issues.....	35

3.2 Research design .....	36
3.3 Data availability and collection .....	37
3.3.1 Meteorological data .....	38
3.3.2 Discharge data.....	38
3.4 Evaluation and comparison of methods of estimation of $E_{TO}$ .....	38
3.5 Evaluation of evapotranspiration using Surface Energy Balance System .....	40
3.5.1 MODIS image acquisition and calibration.....	40
3.6 Estimating the spatial and temporal variation of soil moisture and $E_{TA}$ using TOPMODEL .....	43
3.6.1 TOPMODEL parameters .....	44
3.6.2 DEM hydro processing .....	44
3.6.3 Preparation of TOPMODEL inputs .....	45
3.6.4 TOPMODEL calibration.....	46
3.6.5 TOPMODEL validation.....	46
3.6.6 Soil moisture estimation using TOPMODEL .....	47
3.7 Assessment of Water Availability and Consumption in the Mbire District.....	48
4. RESULTS AND DISCUSSION .....	49
4.1 Evaluation and comparison of point based methods of estimation of potential $E_{TO}$ .....	49
4.2 The spatial and temporal variation of $E_{TA}$ in the Mbire District.....	53
4.3 Estimation of the spatial and temporal variation of soil moisture using TOPMODEL .....	57
4.3.1. Spatial variation of terrain input .....	57
4.3.2 The spatial variation of the Wetness Index.....	58
4.3.3 Runoff calibration results for Manyame and Angwa River sub catchments.....	59
4.3.4 The spatial variation of soil moisture using TOPMODEL .....	61
4.4 Assessment of Water Availability in the Mbire District.....	64
4.5 Conclusions.....	65
4.6 Recommendations.....	66
References.....	67
APPENDICES .....	76
Appendix 1: SEBS SCRIPT RUN in ILWIS 3.4 or 3.7.....	76
Appendix 2: SOIL MOISTURE SETUP IN THE MUSENGEZI SUB-CATCHMENT .....	79
Appendix 3: AUTOMATED WEATHER STATION SETUP AT CHIDODO CLINIC.....	80

## **List of Tables**

Table 2-1: Methods of calculating hydrological elements .....	28
Table 2-2: Precipitation methods and their descriptions .....	28
Table 3-1: Data sources and datasets used in each objective .....	37
Table 3-2: Methods of estimating evapotranspiration .....	39
Table 3-3: MODIS bands that were used in this research .....	40
Table 3-4: Parameter values used and their definitions.....	44
Table 4-1: Evaluation of the various methods for calculating mean daily ETp .....	50
Table 4-2: The mean $E_{TA}$ from 2005 to 2015 for the Mbire District.....	53
Table 4-3: The mean $E_{TA}$ from October 2015 to February 2016.....	54
Table 4-4: Actual evapotranspiration results comparing SEBS/TOPMODEL to $E_{TO}$ .....	57
Table 4-5: Model parameters and model efficiency after validation.....	60
Table 4-6: A water balance from 4/11/2015-31/01/2016 (SEBS $E_{TA}$ ).....	65
Table 4-7: A water balance from 4/11/2015-31/01/2016 (TOPMODEL $E_{TA}$ ).....	65

## **List of Figures**

Fig 3-1: Map of Mbire district with major settlement, weather stations and rivers .....	33
Fig 3-2: Temperature variation for November at Mushumbi, Mbire District.....	34
Fig 3-3: In Air Density variation for November at Mushumbi, Mbire District .....	34
Fig 3-4: Humidity variation for November at Mushumbi, Mbire District .....	35
Fig 4-1: The relationship between ETp of Penman Monteith and Hargreaves equation .....	51
Fig 4-2: The relationship between ETp of Penman Monteith and Turc equation.....	51
Fig 4-3: The relationship between ETp of Penman Monteith and Priestley-Taylor equation .....	52
Fig 4-5: The relationship between ETp of Penman Monteith and Penman equation .....	53
Fig 4-6: The variation of $E_{TA}$ from 2005 to 2015 in the month of August .....	54
Fig 4-7: $E_{TA}$ of the Mbire District in Nov 2015-Mar 2016 .....	55
Fig 4-8: $E_{TA}$ of the Mbire District in October from 2007- 2014 .....	56
Fig 4-9: Hydro-processing (a) distance map (b) flow accumulation (c) flow direction for Manyame .....	57
Fig 4-10: Hydro-processing (a) distance map(b) flow accumulation (c) flow direction for Angwa .....	58
Fig 4-11: Hydro-processing (a) distance map (b) flow accumulation (c) flow direction for Musengezi ...	58
Fig 4-12: Wetness Index histogram and map for Musengezi River sub-catchment .....	59
Fig 4-13: Comparison between simulated and observed runoff for Manyame sub catchment.....	61
Fig 4-14: Soil moisture simulated for Musengezi, Manyame & Angwa .....	62
Fig 4-15: Soil moisture from the data logger for Musengezi sub catchment.....	63
Fig 4-16: Soil moisture simulated by TOPMODEL for Musengezi sub catchment .....	64

## **LIST OF SYMBOLS AND ABBREVIATIONS**

ASTER	Advanced Space borne Thermal Emission and Reflection Radiometer
AVC	Available Water Capacity
DEM	Digital Elevation Model
ET <sub>a</sub>	Actual Evapotranspiration
ET <sub>p</sub>	Potential Evapotranspiration
FAO	Food and Agriculture Organization (United Nations)
GPS	Global Positioning System
ILWIS	Integrated Land and Water Information System
K	Kelvin
Landsat	Land Satellite
MODIS	Moderate Resolution Imaging Spectroradiometer
n	Manning's coefficient
NSE	Nash-Sutcliffe's coefficient of efficiency
PBIAS	percent bias
PDQ	percentage difference of runoff
PMW	Potential maximum wetness
SEBS	Surface Energy Balance System
RS	Remote sensing
RDC	Rural District Council
TM	Thematic Mapper
TOPMODEL	Topographic Model
USGS	United States Geological Survey
WMO	World Meteorological Organisation
ZIMASSET	Zimbabwe Agenda for Socio Economic Transformation
ZINWA	Zimbabwe National Water Authority

## **Dedication**

This work is dedicated to Mr and Mrs Samboko

## **Acknowledgements**

Special thanks to my sponsors, Mr. and Mrs. Samboko. I also gratefully acknowledge my supervisors Mr. Webster Gumindoga and Dr. Eng. Hodson Makurira for their generous help and contribution to my ability to complete the work. A special thanks to the Eco-Hydro Phase 2 Project which provided funding for field work data collection.

I would like thank Eng. S. Musoni and Dr. W. Gwenzi for equipping me with the relevant water resources background which inspired me specialize in the area. I also wish to extend my gratitude to my colleagues, 2015-2016 MSc. WREM & IWRM class, I appreciate your support.

## **ABSTRACT**

Water availability and consumption assessments are important for integrated water resources management. Such assessments are usually hindered by the lack of hydro-meteorological data to close the water balance. Remote sensing based methods and hydrological modelling techniques provide tools to obtain estimates of spatial and temporal variation of key water balance components such as evaporation, transpiration and soil moisture which account for about 65 % of the global water budget. In this study, twenty atmospherically corrected MODIS images taken between 2005 and 2015 in the Mbire District in Zimbabwe were processed using the Surface Energy Balance System (SEBS) algorithm to determine the actual evapotranspiration ( $E_{TA}$ ). The study revealed an increasing trend of actual evapotranspiration from 2005 to 2015, with values of  $E_{TA}$  of around 7 mm/day being observed in the densely forested regions as compared to 3 mm/day for grassland. Results also showed that the SEBS estimated mean  $E_{TA}$  values (3.79 mm/day) were within reasonable range of the mean Potential ET (3.31 mm/day) for the 3 automatic stations which were setup in the district during the period of study. The Topographic driven rainfall runoff model (TOPMODEL) whose land surface inputs were obtained from remote sensing techniques was calibrated with runoff data and was extended to simulate soil moisture patterns as well as  $E_{TA}$  from September 2008 to August 2010. The model simulation yielded Nash Sutcliffe (NSE) values of 0.4 and 0.1 for Manyame and Angwa respectively during the calibration period. Results for soil moisture estimation by TOPMODEL showed high levels of soil moisture (mean value of 80 %) along river channels, valleys and floodplains. The point to pixel comparison of soil moisture simulated by the model and the one retrieved by the data logger at Chidodo station showed a difference of 12 %. A water balance analysis for the basin was conducted by subtracting all outflows from the basin inflows, the inputs driven by SEBS and/or TOPMODEL. Results of the precipitation and evapotranspiration estimates reveal that, the Mbire District received an average of 4.37 mm/day and 4.66 mm/day respectively from November to the end of March 2016. Refinement of the analysis was achieved by dividing the Mbire District into 3 hydrological sub-catchments and this saw an improved SEBS derived water balance closure by 7.2 %, 16.5 % and 12.8 % as compared to 11 %, 20 % and 16.1 % by TOPMODEL for the Angwa, Manyame and Musengezi basins respectively. Ultimately a combination of GIS, hydrological modelling and remote sensing techniques have proven to be an affordable and efficient means of determining water balance parameters, closure of water balance, determine water availability and hence facilitate easier and more efficient analyses in areas where point data may be scarce or unavailable.

**Key words:** Actual Evapotranspiration, Data loggers GIS, Middle Zambezi Basin, TOPMODEL, Soil moisture, Wetness Index.

## **1. INTRODUCTION**

### **1.1 Background**

The limited availability of water poses a challenge to water resources development and economic activities that depend on water resources such as agriculture. This is principally critical in arid and semi-arid regions where water scarcity poses a severe constraint to food production, health and sanitation issues (De Fraiture et al., 2003). In most cases there is a lack of data on the actual usage and availability of water and this hampers sustainable management and development of water resources. For effective water management, quantification of the water balance components is fundamental to understanding the hydrological behavior of a system. In the assessment of water resources and derivation of the water balance, it is important to understand the spatial and temporal dynamics of the anchors of the water balance such as evapotranspiration, soil moisture, and runoff (Beven, 1997; Ukkola and Prentice, 2013). This is critical for planning and development of water resources infrastructure and crop growth

Quantifying the water balance in arid and semi-arid regions is critical as the scarcity of water as worsened by climatic variability and land use change lead to conflicts associated with water usage (Troch, 2000). This becomes more complicated in un-gauged basins where the inflows as well outflows are not known (Penkova and Shiklomanov, 2002; Yanmin et al., 2014). Remote sensing data presents an interesting opportunity as it allows for the quantification of key water balance components such as evapotranspiration. The above is not only important for water resources planning and management in the Mbire District but for downstream catchments.

A fundamental part of this process is the need and ability to spatially quantify actual evapotranspiration in space and time. This need is very critical in water limited environments because, in these environments, evapotranspiration is a major component of the water balance. This comes on the backdrop of evapotranspiration contributing 65 % of the global water balance (Ukkola and Prentice, 2013). In the Zambezi Basin floodplain, determination of evapotranspiration is critical for crop growth as crop water requirements are greatly affected by the prevailing evapotranspiration levels (Maina et al., 2014). The government of Zimbabwe is promoting establishment of irrigation schemes through an irrigation Master Plan which also includes the Mbire District in the Middle Zambezi Basin. Farmers in the Mbire District rely on

recession farming. It is essential for the farmers in the Mbire District of the Zambezi basin to be able to use evapotranspiration data estimated on a spatial and temporal scale (Salama et al., 2015). The above is important for their financial planning, crop selection, irrigation development and irrigation scheduling for the farmers.

The conventional methods of determining evapotranspiration are usually point based approaches. These include Hargreaves, Makkink, Penman, Priestley, FAO Penman–Monteith, Thornthwaite, and Taylor and equations. The limitations of these methods are time of measurement, number of sites, unknown accuracy as well as different periods of measurement. In the Mbire District, point based evapotranspiration estimates are not only inadequate but also do not deal with the need to implement effective water resources such as, monitoring, system evaluation and planning (Hassan et al., 2003). The alternative to point based methods is remote sensing based modelling techniques. These methods are there to tackle key challenges in management water resources in hydrological areas such as the Mbire District that are physically heterogeneous. The losses in flux attributable to the different land cover types in the catchment are unknown, as such this lack of information affects the determination of the water balance necessary for crop production (Rwasoka et al., 2011). In addition remote sensing based approaches allow for water balance components to be determined spatially at non-conventional scales such as administrative boundaries. As such the water available for consumption can easily be determined in space and in time and can be related to changes in demand and supply in a unit such as a district (Yanmin et al., 2014).

Gaining an appreciation for spatial and temporal variations of soil moisture is important for determining a water balance for any catchment as soil moisture determines the crop selection, crop water requirement and irrigation design. Soil moisture variations in time and space are controlled by many factors, such as soil texture, topography and vegetation (Yang et al., 2012). Soil moisture determines how incoming solar radiation will be partitioned into sensible heat flux and latent heat flux. It also determines how incoming rainfall will be partitioned into surface runoff and subsurface infiltration (Yu et al., 2001a). Soil moisture is thus one of the key parameters governing interactions among atmosphere, land surface, and ground water. Therefore, its determination on a spatial and temporal scale cannot be overlooked for the successful implementation of an integrated water resources management program.

Soil moisture measured by point based methods has disadvantages of being irrelevant for areas far away from the point of measurements. The point based measurements are usually biased, inaccurate, strongly depend on the topography of the area and lack the spatial and temporal variation needed especially when soil moisture data is needed at large scale domains. Soil moisture at large scales can be estimated by hydrologic modeling and remote sensing. Remote sensing methods for soil moisture retrieval, whilst they provide spatial coverage of some variables useful for hydrologic models, however, they do not provide a soil moisture column-average (Capehart and Carlson, 1997). With appropriate input data, hydrologic models can provide an estimation of the spatial distribution of soil moisture for water balance estimates of any area.

## **1.2 Problem Statement**

Water resources are central for the livelihoods of people who live in the Zambezi basin particularly the Mbire District in Zimbabwe. Determination of key water balance components such as evapotranspiration is important since evapotranspiration contributes 65 % of the global water balance in semi-arid areas and is directly linked to other water balance components such as rainfall and soil moisture. Point based measuring methods are often used to quantify evapotranspiration and soil moisture. The spatial and temporal variations of evapotranspiration and soil moisture are not accounted for by these point based approaches. This is due to the fact that with point based measurements there is a limited time of measurement, limited number of sites, unknown accuracy as well as different periods of measurement. There is an urgent need for remote sensing based approaches for evapotranspiration and soil moisture determination for near real time accounting of the water balance of the Mbire District which is part of the Zambezi basin catchment area. Coupled with modelling approaches such as hydrological modelling techniques, progress can be made with respect to planning for crop production and irrigation development in the Mbire District.

Together with improved evapotranspiration estimates, soil moisture plays a crucial role in several land surface processes, affects vegetation and plant growth and contributes to the interaction between land surface and atmosphere (Dente, 2016). Because of this importance, there is an urgent need to accurately retrieve these two key water balance components in space and time. The Mbire District becomes an interesting avenue to test the different soil moisture and

evapotranspiration retrieval techniques, coupled with in situ measurements. This is because the above water balance components play a central role in the livelihoods of the Mbire District residents who depend on both rain-fed and recession farming. Obtaining reliable and representative soil moisture and evapotranspiration estimates in the District and in the Middle Zambezi basin at large is a major challenge due to low number of gauging equipment, poor spatial distribution of the gauges, and variation in topography with climatic gradients.

### **1.3 Justification**

According to the Food and Agriculture Organisation of the UN, the right to adequate food is a universal human right that is realized when all people have physical and economic access at all times to adequate food or the means for its procurement, without discrimination of any kind (FAO, 1996). In addition the thrust of the Food Security and Nutrition Cluster in the Zimbabwe Agenda for Sustainable Socio-Economic transformation is to “create a self- sufficient and food surplus economy” (ZIMASSET, 2013).

To be able to fully assess water availability for improving production for farmers in the Mbire it is important to map evapotranspiration both on a temporal and spatial scale. Farming in semi-arid areas such as the Mbire requires knowledge of key hydrological components necessary for water balancing such as evapotranspiration. An Irrigation Master Plan currently being proposed by the government of Zimbabwe would be greatly complimented by the mapping of evapotranspiration and soil moisture for crop water requirement purposes. The existing point based methods of determining evapotranspiration and soil moisture have proven to be incapable of spatial and temporal mapping thus the need to use a GIS based algorithms such as SEBS and TOPMODEL.

### **1.4 Hypothesis**

Remote sensing based methods can improve assessment of water availability

## **1.5 Main Objective**

To determine the water balance for the Mbire District of Zimbabwe using a remote sensing based approach.

### **1.5.1 Specific Objectives**

1. To evaluate and compare five methods of potential evapotranspiration estimation.
2. To determine the spatial and temporal variation of actual evapotranspiration using the Surface Energy Balance System and the TOPMODEL based algorithm
3. To estimate the temporal and spatial variation of soil moisture in Mbire District using TOPMODEL
4. To conduct a water balance of the Mbire District

## **1.6 Thesis structure**

The study consists of the following structures; the first chapter contains the background and introduction, the problem statement, justification and objectives of the study. Chapter Two contains literature review on evapotranspiration, surface energy balance system (SEBS), TOPMODEL and other methods. The third chapter has a detailed study area as well as the methodology which was used for data collection and analysis. Chapter Four presents the results and discussions on comparison of the methods of calculating potential evapotranspiration, use of SEBS and TOPMODEL to determine actual evapotranspiration estimation and determination of soil moisture using TOPMODEL in the Mbire District. The fifth chapter has the conclusions and recommendations from the thesis

## **2. LITERATURE REVIEW**

### **2.1 Water balance of semi-arid areas**

Water balance is critical in semi-arid regions as it can be used to analyse the hydrology of an area. It also enables one to get an assessment of the quality of the data and detect discrepancies. Water balance assessment can be conducted for both large and small areas. The analysis of a catchment can be as short as one second and as long as many years. Comparing one catchment with another of similar hydro-meteorological data will point out whether there are any differences. Riparian areas along streams and rivers are very distinct environments and usually have greater soil moisture and soil fertility than the surrounding areas.

### **2.2 Evapotranspiration**

Evapotranspiration is made out of two main components, potential and actual. Actual evapotranspiration ( $E_{TA}$ ) is the quantity of water that is actually removed from a surface due to the processes of evaporation and transpiration, potential is the amount removed from the surface in abundant water situations (Pidwirny, 2006).

#### **2.2.1 Estimation of evapotranspiration**

There are many methods for estimating potential and actual evapotranspiration ( $E_{TA}$ ). These are classified based on data requirements (Dingman, 2002). They are clustered as radiation based, temperature based, combination and pan methods. In the case of  $E_{TA}$  the widely used methods are the water balance approaches. The energy balance deals with phenomena such as the Bowen ratio conservation of energy, the Penman-Monteith and the Eddy correlation.

#### **2.2.2 Methods of estimating potential evapotranspiration**

There are many methods that have been proposed to estimate Potential evapotranspiration ( $E_{TO}$ ) in the world. Some of the most popular ones are discussed in here (Allen and Pereira, 1998).

##### ***Penman-Monteith Method***

For daily estimate of potential evapotranspiration the Food and Agricultural Organization (FAO) Penman-Monteith method was used (Allen and Pereira, 1998).

$$ET_0 = \frac{0.408(R_n - G) + \gamma \frac{900}{T + 273} u (e_s - e_a)}{\Delta + \gamma(1 + 0.34u)} \quad (1)$$

where;

$ET_0$	=	Daily reference crop evapotranspiration [mm/day]
$R_n$	=	Net radiation flux [ $\text{MJ m}^2/\text{day}$ ]
$G$	=	Heat flux density into the soil, [ $\text{MJ}/\text{m}^2/\text{day}$ ]
$T$	=	Mean daily air temperature [ $^{\circ}\text{C}$ ]
$\gamma$	=	Psychometric constant [ $\text{kPa}/^{\circ}\text{C}$ ]
$U$	=	Wind speed measured at 2m height [m/s]
$e_s$	=	Saturation vapour pressure [kPa]
$e_a$	=	Actual vapour pressure [kPa]
$RH$	=	Relative humidity [%]
$e_s - e_a$	=	Saturation vapour pressure deficit [kPa]
$\Delta$	=	Slope of saturation vapour pressure curve [ $\text{kPa } ^{\circ}\text{C}$ ]

### ***Thornthwaite formula***

This particular formula was based on mainly temperature with slight adjustments being made with respect to the number of daylight hours. An estimate of the potential evapotranspiration, calculated on monthly basis is given in Equation 2.

$$E_{T0} = 16f\left(\frac{10t_n}{j}\right)^a \quad (2)$$

where;

$J$	=	Monthly heat index
$A$	=	Cubic function of $j$
$t_n$	=	Monthly mean temperature

### ***Blaney-Criddle formula***

This is an empirical model which requires only mean daily temperatures over each month to calculate Potential evapotranspiration ( $E_{TO}$ ) as in Equation 3.

$$PET = a + b(p(0.46T_{mean} + 8.13)) \quad (3)$$

where;

a = Calibrated parameter (functions of the minimum daily relative humidity)

b = Calibrated parameter (functions of the minimum daily relative humidity)

$T_{mean}$  = Mean daily temperature [Kelvin's]

P = Annual mean daily daytime hours [hrs]

### ***Hargreaves Formula***

This is an empirical equation which needs solar radiation and temperature only.

$$ET_o = 0.0023R_N(T_{mean} + 17.8)(T_{max} - T_{min})^{\wedge}HE \quad (4)$$

where;

$R_n$  = extra-terrestrial solar radiation.

$T_{max}$  = maximum daily air temperature ( $^{\circ}C$ ),

$T_{min}$  = minimum daily air temperature ( $^{\circ}C$ )

$T_{mean}$  = mean daily temperature ( $^{\circ}C$ )

### **2.2.3 Remote Sensing approaches in estimating evapotranspiration**

RS quantification is based on measurements of reflectance and emitted electromagnetic radiation from the Earth's surface. In the estimation of atmospheric turbulent fluxes there are 2 basic physical principles. These are the conservation of energy as well as the turbulent transport is considered (Su, 2002). Conservation of energy is in fact the basis of the surface energy balance approach.

The net radiation is the sum of all incoming and outgoing radiation of short and long wavelengths (Allen and Pereira, 1998).

There are a number of algorithms that use RS imageries which have been developed for evapotranspiration. These algorithms are Disaggregated Atmosphere Land Exchange Inverse model (DisALEXI), SEBAL, Simplified Surface Energy Balance Index (S-SEBI), and SEBS (Bastiaanssen et al., 1998; Norman, 2003; Roerink et al., 2000; Su, 2002). It is indeed possible to estimate actual evapotranspiration in combination with daily meteorological (Immerzeel et al., 2006).

### ***Disaggregated Atmosphere Land Exchange Inverse model***

The DisALEXI algorithm is made up of two-steps. The ALEXI is executed at a resolution of 5 km so as to estimate the temperature of the air. This is at the boundary between the land surface and sub models. Holding the air temperature constant at the ALEXI value, TSM is used for vegetation and temperature (Norman, 2003). ALEXI-derived vertical temperature gradient is preserved in the disaggregation stage by correcting the high-resolution radiometric temperature field for biases so as to produce an average which is consistent with the 5-km temperature data. The high resolution flux outputs predictions can then be re-aggregated and compared with observations from the tower; this is assuming a certain weighting function describing the surface source footprint. The current techniques which are used in the estimation of flux footprint distributions are made up of two classes. These are the analytical and Lagrangian models. The more rigorous Lagrangian needs detailed specifications which may not be available in many study areas (Leclerc and Thurtell, 1990). The DisALEXI approach assumes that horizontal fluxes are small in comparison with vertical fluxes (Wieringa, 1986). In heterogeneous environments both these assumptions may be violated, small-scale surface atmospheric coupling and advection can become substantial. DisALEXI has been used to determine evapotranspiration successfully in the United States taking the Landsat spatial scale into account (Anderson et al., 2012).

### ***Surface Energy Balance Algorithm for Land (SEBAL)***

The SEBAL is a parameterization of the energy balance and surface fluxes based on spectral satellite measurements. SEBAL requires certain spatially distributed input data which includes Visible, Near-infrared and Thermal infrared from satellite imageries. The SEBAL algorithm

deduces the radiation, heat and evaporative fluxes through an iterative and feedback-based procedure. One of its most significant benefits is that it requires little field information and computes most crucial hydro meteorological parameters (Bastiaanssen et al., 1998). Computation of the energy balance during the satellite overpass and the integrated twenty four hour fluxes are computed on pixel by pixel foundation. The SEBAL has several steps for computational of images and calculates the  $E_{TA}$ . Having ignored energy requirements for photosynthesis and the heat storage in vegetation, SEBAL reads as:

$$R_n = G_0 + H + LE \quad (5)$$

where;

$R_n$  = Net radiation absorbed at the land surface ( $W/m^2$ )

$G_0$  = Soil heat flux to warm or cool the soil ( $W/m^2$ )

$H$  = Sensible heat flux to warm or cool the atmosphere ( $W/m^2$ )

$LE$  = Latent heat flux associated with evaporation of water from soil ( $W/m^2$ )

The soil heat flux requires the following variables for computation: surface temperature, albedo and the normalized vegetation index (NDVI). This method has been used to determine evapotranspiration in Iran where it yielded good results. The study concluded that the SEBAL model is highly useful in determining evapotranspiration by means of meteorological data and remote sensing techniques (Matinfar, 2012).

### ***Simplified Surface Energy Balance Index***

The main difference between S-SEBI and SEBAL is that S-SEBI calculates heat flux using the evaporative fraction, while SEBAL calculates using the surface energy balance residual. algorithm uses the evaporative fraction ( $\bar{A}$ ) theory through parameterization to solve the surface energy balance (Roerink et al., 2000):

$$\bar{A} = \frac{T_H - T_S}{T_H - T_{\lambda E}} \quad (6)$$

where;

- $T_S$  = Land surface temperature,  
 $T_H$  = Temperature of maximum sensible heat flux pixels  
 $T_{\lambda E}$  = Temperature of the maximum latent heat flux

$$\bar{A} = \frac{a_H + b_H \alpha - T_S}{a_H - a_{\lambda E} + (b_H - b_{\lambda E}) \alpha} \quad (7)$$

$\bar{A}$  was calculated as: The H and  $\lambda E$  are obtained using the available energy and  $\bar{A}$ , according to:

$$H = (1 - \Lambda)(R_n - G) \quad (8)$$

And

$$\lambda ET = \Lambda(R_n - G) \quad (9)$$

Finally, the daily ET estimation by S-SEBI is based on the theory that the instantaneous evaporative fraction  $\Lambda_i$  is equal to the daily evaporative fraction  $\Lambda_d$ :

$$\Lambda_i = \Lambda_d = \frac{\lambda ET_i}{R_{ni} - G_i} = \frac{\lambda ET_d}{R_{nd} - G_d} \quad (10)$$

Given that the integrated daily soil heat flux is approximately equal to zero with respect to Allen and Pereira (1998), the daily evapotranspiration can then be calculated by:

$$ET = \lambda ET_i \frac{R_{nd}}{\lambda R_{ni}} \quad (11)$$

S-SEBI has been used in Brazil to determine evapotranspiration for cotton. In this study S-SEBI gave results had a high correlation with SEBAL  $E_{TA}$  results for the same study area despite being consistently lower than SEBAL (Santos et al., 2010).

### **2.3 Surface Energy Balance System algorithm theory**

The SEBS algorithm determines turbulent heat flux by employing meteorological and satellite spectral reflectance and radiance data (Su, 2002). SEBS algorithm is based on equation 12 as shown:

$$R_n = G_0 + H + \lambda E \quad (12)$$

where;

$R_n$	=	Net radiation [ $\text{W m}^{-2}$ ]
$G_0$	=	Soil heat flux [ $\text{W m}^{-2}$ ]
$H$	=	Sensible heat flux [ $\text{W m}^{-2}$ ]
$\lambda E$	=	Latent heat flux [ $\text{W m}^{-2}$ ]
$\lambda$	=	Latent heat of vaporisation [ $\text{J kg}^{-1}$ ]
$E$	=	Evapotranspiration. [mm/day]

$R_n$  is given by:

$$R_n = (1 - \alpha) \cdot R_{\text{swd}} + \varepsilon \cdot R_{\text{ldw}} - \varepsilon \cdot \sigma \cdot T_0^4 \quad (13)$$

where;

$\alpha$	=	Albedo
$R_{\text{swd}}$	=	Downward shortwave radiation [ $\text{W m}^{-2}$ ]
$R_{\text{ldw}}$	=	Downward long wave radiation [ $\text{W m}^{-2}$ ]
$\varepsilon$	=	Emissivity
$\sigma$	=	Stefan–Boltzmann constant [ $\text{W m}^{-2}\text{K}^{-4}$ ]
$T_0$	=	Surface temperature [K]

Energy that goes into the soil, the soil heat flux is calculated taking into account fractional vegetation cover,  $f_c$ , with constants for full vegetation canopy and bare soil (Kustas and Daughtry, 1990; Monteith, 1981). The equation is:

$$G_0 = R_n \cdot [\Gamma_c + (1 - f_c) \cdot (\Gamma_s - \Gamma_c)] \quad (14)$$

where;

$\Gamma_c$  = Full vegetation cover

$\Gamma_s$  = Bare soil

To derive sensible heat flux (H), a similar theory is used. Since the measurements are done in the Atmospheric Surface Layer (ASL), the Monin–Obukhov Similarity (MOS) functions are used supported by stability correction (Beljaars and Holtslag, 1991; Monin and Obukhov, 1954; van den Hurk and Holtslag, 1997).

The value of H is then determined by considering the limiting values under the dry and wet limit. At the dry moisture limit, latent heat ( $\lambda E_{dry}$ ) becomes zero and sensible heat ( $H_{dry}$ ) would be at its maximum. By definition, from Equation 12, it follows that:

$$\lambda E_{dry} = R_n - G_0 - H_{dry} = 0 \text{ or } H_{dry} = R_n - G_0 \quad (15)$$

Given that sensible heat flux is ( $H_{wet}$ ) and evapotranspiration is ( $\lambda E_{wet}$ ), limited only by the available energy. It follows therefore that:

$$\lambda E_{wet} = R_n - G_0 - H_{wet} \text{ or } H_{wet} = R_n - G_0 - \lambda E_{wet} \quad (16)$$

K is evaporative fraction which it follows that:

$$\lambda = \frac{\lambda E}{R_n - G} \quad (17)$$

By inverting Eq. (17), latent heat was determined by  $\lambda E = \Lambda (R_n - G_0)$

The latent heat flux accounts for the total vapour flux into the atmosphere expressed. Actual evapotranspiration (E) was then calculated by  $E = \lambda E / \lambda \cdot \rho_w$ , where E is the actual evapotranspiration [ $\text{mms}^{-2}$ ],  $\lambda$  is the latent heat of vaporisation [ $\text{J kg}^{-1}$ ], and  $\rho_w$  is the density of water [ $\text{kg m}^{-3}$ ] (Jia et al., 2009).

Satellite images represent an instantaneous observation in time and hence E is initially  $\text{mm s}^{-1}$ . Daily evapotranspiration is therefore determined based on the evaporative fraction. It is assumed

to remain constant throughout the day (Jia et al., 2009; Sugita and Brutsaert, 1991). Total daily evapotranspiration is therefore given by:

$$\begin{aligned} E_{\text{daily}} &= \sum_{i=0}^{24} A \cdot \frac{R_n - G}{\lambda \cdot \rho_w} & (18) \\ &= 24 \text{ h} \cdot 3600(\text{s}) \cdot \left[ \Lambda \cdot \frac{R_{\text{ndaily}} - G_{\text{daily}}}{\lambda \rho_w} \right] \\ &= 8.6 \times 10^7 \cdot \left[ \frac{R_{\text{ndaily}} - G_{\text{daily}}}{\lambda \rho_w} \right] \end{aligned}$$

where;

- $E_{\text{daily}}$  = Daily evapotranspiration [ $\text{mm d}^{-1}$ ],
- $R_n$  = Net radiation
- $G$  = Soil heat flux
- $R_{\text{ndaily}}$  = Average net radiation
- $G_{\text{daily}}$  = Soil surface heat flux
- $K$  = Evaporative fraction,
- $q$  = Density of water [ $\text{kg m}^{-3}$ ]
- $k$  = Latent heat of vaporisation [ $\text{J kg}^{-1}$ ]

with a numeric value of  $2.47 \times 10^6$  (Jia et al., 2009; Sugita and Brutsaert, 1991).

### **2.3.1 Roughness**

Surface conditions are characterised by roughness terms. Roughness height represents heat transfer,  $z_{\text{oh}}$ , was derived from a certain model (Su, 2002).  $kB_s^{-1}$  is the term that applies for bare land (Brutsaert, 1982).

$$KB^{-1} = \frac{KC_d}{4C_t \cdot \frac{u}{u(h)} (1 - e^{-n_{ec}/2})} \cdot f_c^2 + 2f_c f_s \frac{k \cdot \frac{u_*}{u(h)} \cdot \frac{z_{om}}{h}}{C_t^*} + kB_s^{-1} f_s^2 \quad (19)$$

where

$f_c$	=	Fractional canopy coverage
$f_s$	=	Fraction of non-vegetated soil
$(1 - f_c) \cdot C_t$	=	Heat transfer coefficients for a leaf
$C_t^*$	=	Heat transfer coefficients for soil.
$n_{ec}$	=	Canopy wind speed extinction coefficient.

The roughness height for heat transfer  $z_{oh}$  was then derived from:

$$z_{oh} = \left( \frac{z_{om}}{\exp(kB^{-1})} \right) \quad (20)$$

where;

$z_{om}$  = roughness length for momentum transfer.

### 2.3.2 Advection-aridity evapotranspiration method

The advection-aridity method is used to determine actual evapotranspiration using meteorological data from Mushumbi, Chidodo and Masoka automated weather stations. The daily advection-aridity method is chosen on the basis of the time-step allowed comparison with SEBS results (Brutsaert and Stricker, 1979). Advection-aridity has been utilised in many studies to estimate  $E_{TA}$  together with techniques with good results (Gonzales and Parodi, 2010; Hobbins et al., 2001; Liu et al., 2010; Ramírez et al., 2005). Rwasoka (2010) found that the advection aridity equation had good predictive power at daily time steps if compared to eddy covariance. The advection-aridity equation used, after Brutsaert and Stricker (1979) as follows:

$$E_{TA} = (2\alpha_e - 1) \frac{\Delta}{\Delta + \gamma} Q_{ne} - \frac{\gamma}{\Delta + \gamma} E_A \quad (21)$$

where;

$E_{TA}$	=	Actual evapotranspiration [mm/d],
$Q_{ne}$	=	Ratio of $R_n$
$\Delta$	=	Slope of vapour pressure versus temperature [kPa .C <sup>-1</sup> ]
$\gamma$	=	Psychometric constant [kPa .C <sup>-1</sup> ]

$E_A$  is the drying power of air (Brutsaert, 2005; Brutsaert and Stricker, 1979). The advection effects were scaled by the aerodynamic vapour transfer term  $E_A$  expressed as:

$$E_A = f(u_r)(e_s - e_a) \quad (22)$$

where;

$$\begin{aligned} f(u_r) &= \text{Wind function,} \\ e_s &= \text{Saturation vapour pressure} \\ e_a &= \text{Actual vapour pressure mmHg (Brutsaert and Stricker, 1979).} \end{aligned}$$

The wind function used is a Stelling-type standard equation stated as:

$$f(u_2) = 0.26(1 + 0.54u_2) \quad (23)$$

where;

$$u_2 = \text{mean wind speed [ms}^{-1}\text{].}$$

SEBS is recommended over other methods because it is a physically based model which can be applied to various conditions. It has been applied in many different heterogeneous areas (Liou and Kar, 2014). SEBS also minimizes uncertainty in terms of meteorological variables as well as surface temperature (Eden, 2012). Finally SEBS can model evapotranspiration for long and short time steps/periods as well as over a wide set of meteorological conditions (Glenn et al., 2007).

#### **2.4 Hydrological modeling techniques for water balance assessments**

Computer based models have been developed for rainfall-runoff simulation by hydrological researchers since the early 1960s (Crawford and Linsley, 1966). This has resulted in the increased use and development of models. In accordance with (Beck, 1991) the following brief descriptions of metric, conceptual, and physically based rainfall-runoff models are described.

Metric or empirical models characterize runoff by direct observations; they are formulated with little consideration of the hydrological cycle. Physically based models simulate hydrological responses based on the governing hydrodynamics and transport equations. The governing equations for a physically based model are measurable parameters and variables (Beven, 1983).

### **2.4.1 Hydrologic Modeling System**

The HEC-HMS model is designed to simulate the precipitation and runoff process of dendritic watershed systems. It also simulates soil moisture accounting (SMA) algorithms which in turn accounts for watershed's soil moisture balance over a long-term period of time (Roy et al., 2013). It is also suitable for simulating daily, monthly, and seasonal stream flow. The SMA algorithm takes explicit account of all runoff components inclusive of direct runoff as well as indirect runoff (Ponce, 1989). The inputs required by the model include daily rainfall, soil condition and other hydro meteorological data.

HEC-HMS needs three sets of input data to build the model up. The first set of inputs is for catchment model which deals with simulation of runoff. The second set is meteorological model which defines the characteristics of precipitation in any form. Finally is the Control Specification which specifies the starting and ending date of the model plus the intermission of input data. Certain terrain features need to be added to the model, these are terrain characteristics of the catchment as well as the streams.

Sub-catchments and hydrologic parameters which include slope and length should be recognized. The level of connectivity in the segments outlines which element is upstream or downstream. The catchment model is introduced to simulate the sub-catchment through calculating the water losses which occur through infiltration, water delivery through channels and calculating excess overflow.

Meteorological models use several methods to deal with precipitation and evaporation. The type of model used depends on the type of available data, to introduce evaporation and precipitation. Control specification defines the particular time of starting and completion of the simulation as well as calculation time intermissions (HEC, 2006).

Table 2-1: Methods of calculating hydrological elements

Hydrologic Element	Calculation Type	Method
Sub-basin	Loss Rate	Deficit and constant rate (DC)
		Exponential
		Green and Ampt
		Gridded DC
		Gridded SCS CN
		Gridded SMA
		Initial and constant rate
		Gridded SCS Curve Number CN
		Soil moisture accounting (SMA)
	Transform	Clark s UH
		Kinematic wave
		ModClark
		SCS UH
		Snyder s UH
		User-specified s-graph
		User-specified unit hydrograph (UH)
	Base-flow	Bounded recession
		Constant monthly
		Linear reservoir
Recession		
Reach		Kinematic wave
		Lag
		Modified Puls
		Muskingum

Table 2-2: Precipitation methods and their descriptions

Precipitation Methods	Description
Frequency storm	Used to develop a precipitation event where depths for various durations within the storm have a consistent exceedance probability.
Gage weights	User specified weights applied to precipitation gages
Gridded precipitation	Allows the use of gridded precipitation products, such as NEXRAD radar
Inverse distance	Calculates sub-basin average precipitation by applying an inverse distance squared weighting with gages.
SCS storm	Applies a user specified SCS time distribution to a 24-hour total storm depth.
Specified hyetograph	Applies a user defined hyetograph to a specified sub-basin element.

There are a number of studies which have used HEC-HMS in the process of determining the Water balance. One of these was done in the Chinese River Basin in an arid area similar to the Mbire District. The water balance results revealed a general aridity trend consistent with the expected results and thus proving that HEC-HMS was a good model for water balancing (Moghadas, 2009). Another study on the calibration and validation of HEC-HMS concluded that the model could be used on a wide range of watersheds and catchments as it had been successfully validated with high Nash Sutcliffe values for the stream in India (Roy et al., 2013). Furthermore, a study closer to the Mbire District was successfully conducted to give a water balance on the catchment with settlements upstream of the Cahora Bassa (Phiri, 2011).

#### **2.4.2 HBV Model**

The *Hydrologiska Byrans Vattenbalansavdelning* (HBV) model simulates discharge using rainfall, temperature and evapotranspiration. The model can also be used for flood forecasting (Bloschl et al., 2007). The model has different routines representing soil water and evaporation, groundwater described by three linear reservoir equations (Seibert, 1997). Descriptions of the model are found in literature (Bergstrom, 1992). The model Bergstrom (1976) has been used in many other studies, some of these include computation of hydrological forecasts, design floods or climate change studies.

Some versions of HBV models use a spatial scale of one kilometre and quarter hour time step for precipitation and temperature. HBV is based on five processes through which the rainfall-runoff process is simulated. These are snowmelt, soil moisture, hill-slope, stream and catchment routing. The snow routine depicts snow accumulation and melt by a degree day concept. Soil moisture accounting is calculated as the sum of rainfall and snowmelt. The components are split as a function of  $S_s$ , (Bergstrom, 1976).

HBV, was used successfully to determine actual evapotranspiration in Indian Karkheh River basin. In this study, the HBV driven  $E_{TA}$  was compared to SEBS  $E_{TA}$  giving positively correlated values (Muthuwatta et al., 2009).

$$Q_p = \left(\frac{S_s}{L_s}\right)^\beta \cdot (P_r + M) \quad (24)$$

Where;

$L_s$  = maximum soil moisture storage

$\beta$  = non linearity parameter

The only process that decreases  $S_s$  is evaporation. The potential evaporation,  $E_p$ , by a linear function of the soil moisture of the top layer:

$$E_A = E_p \frac{S_s}{L_p} \text{ if } S_s < L_p \text{ otherwise } E_A = E_p \quad (25)$$

Where;

$L_p$  = limit for potential evaporation.

### **2.4.3 The Curve Number method**

The Natural Resources Conservation Service curve number is generally used to estimate runoff which comes from event rainfall (NRCS, 2001). It is regarded as very simple and convenient. The curve number puts together the effects of soil type, hydrology, land use and land cover. The empirical curve number is a simplification of a conceptual storage index, that being the potential maximum water retention. Curve number is a lumped composite which include all assumptions and approximations used in deriving the relationship between rainfall and runoff. It is the only parameter necessary to relate a rainfall volume to a runoff estimate.

A number of studies have tested the curve number for accuracy to determine its weaknesses (Ponce and Hawkins, 1996). A number of scientists began to question the method on a physical basis (Garen and Moore, 2005). This was after Victor Mockus conceptualized the curve number (Ponce and Hawkins, 1996). The method was heavily criticized as old fashioned, overly simplified and unrealistic. This was mostly in the aspects of flow amounts, runoff source areas, and erosion. Other issues with the method were to do with failure to account for rainfall and runoff temporal variation (Ponce and Hawkins, 1996).

Despite the limitations in the scope of intended applications and numerous problems, curve number method has been used in many diverse environments, including transport models

(Woodward et al., 2002). The curve number approach is used in water balance and storm routing models coupled meteorological and hydrological models (Yu et al., 2001b). Furthermore, the curve number was used specifically to determine a water balance in Wellington Reservoir in India, there was a successful balance with full closure of the water balance (Srinivasan and Poongothai, 2013). This makes it relevant method for the water balance in the Mbire District.

#### **2.4.4 The TOPMODEL Concept**

An increase in availability of Digital Elevation Models has made it possible to integrate GIS with hydrological modeling. In the case of basins with moderate to steep slopes and shallow soils overlying a bed rock that is impermeable, topography has an important role in runoff generation (Beven et al., 1995). The topographic or wetness index otherwise known as the index of hydrological similarity was first introduced by Kirkby et al. (1975) and is the basis for the TOPMODEL rainfall runoff model.

The model makes an effort to explain the hydrologic similarities between points on a catchment in the wetness Index. The grid cells which have similar values of wetness index tend to respond in the same way (Worlock, 1995). TOPMODEL is a semi distributed hydrological model which strikes a balance between simple lumped models and complicated full distribution process models (Robson et al., 1993). TOPMODEL is essentially, a set of tools which put together the parametric and computational efficiency of a lumped approach taking the physical theory into consideration (Beven et al., 1995). The theory of hydrological similarity in a catchment has the TI used as an index similarity basing itself on the rainfall-runoff model (Xiong and Guo, 2004). The wetness index may be used to calculate the effect on rainfall-runoff process by topography. It gives an indication of the soil moisture distribution as well as surface saturation (Muhammed and Enschede, 2012).

The popularity of TOPMODEL can be attributed to its ability to be applied in a wide range of basins. TOPMODEL was used in Karoon River basin of western Iran for rainfall-runoff modelling (Nourani and Mano, 2007). TOPMODEL has been effectively used in the Mekong basin for rainfall-runoff modeling (Takeuchi et al., 2008). Similar to Mbire District conditions, TOPMODEL has been used in dry and humid areas of the Mediterranean regimes (Durand et al., 1992). With respect to Africa, the model has also been used in Buro-borotu basin of Ivory Coast (Quinn et al., 1991). It has also been used successfully in Sinamary river in French Guiana

(Molicova et al., 1997). Some research has been done on interaction between spatial resolution and time step in modeling. HEC-HMS is an example of an event-based model which cannot be used properly for rainfall-runoff modelling (Nourani and Mano, 2007). This is because these models estimation of soil moisture is not possible using models. A full description of TOPMODEL can be found in literature (Beven et al., 1995). TOPMODEL was also applied by Gumindoga for runoff simulation in the Gilgel Abbay Basin in Ethiopia. A satisfactory NSE of 0.788 was obtained (Gumindoga et al., 2014). Closer to the Middle Zambezi Basin, TOPMODEL yielded a satisfactory model performance (NSE of 0.77) in Upper Save Basin in Zimbabwe (Gumindoga et al., 2011).

## **2.5 Determination of water availability and consumption**

Water allocation is dependent on striking a balance between different users which include farmers, environment, household use and industry (Duan and Bastiaanssen, 2013). This balance can be attained by getting information on the variables that determine water availability. In areas such as the Mbire District, there is no sufficient field data for appropriate water resources management. Precipitation and  $E_{TA}$  are both important variables necessary to quantify the availability of water resources appropriately (Moghadas, 2009). When mapping  $E_{TA}$  of large areas it is suggested that remote sensing techniques are utilized (Bandara, 2003; Bastiaanssen and Chandrapala, 2003). In this particular study SEBS is selected to estimate  $E_{TA}$  due to its wide applicability. It has been validated by many studies which conclude that point based data can be compared to SEBS estimation (Jia et al., 2003; Su, 2002; van den Hurk and Holtslag, 1997).

When assessing water availability it is useful to determine the spatial and temporal variability of soil moisture. Rainfall runoff model outputs can be manipulated so as to determine soil moisture variation using. The model has to be validated for runoff simulation before soil moisture was determined (Moges, 2008).

### **3 MATERIALS AND METHODS**

#### **3.1 Description of study area**

The Mbire District is a large area spanning 4 700 km<sup>2</sup>. The coordinates of the area lie between 15.6° to 16.4° South and 30.6° to 31.2° East. The Mbire District has floodplains of the Zambezi basin. The altitude of the area is 400 m above sea level. The Mbire District has a number of rivers draining it. These include the Angwa, Manyame, and Musengezi rivers (LGDA, 2009). Wildlife management areas are the majority of the surrounding areas; in the west of the Mbire District is the Chewore Safari while the Doma Safari is in the significant South. These areas are reserved for hunting and settlement is strictly prohibited (Chenje, 2000).

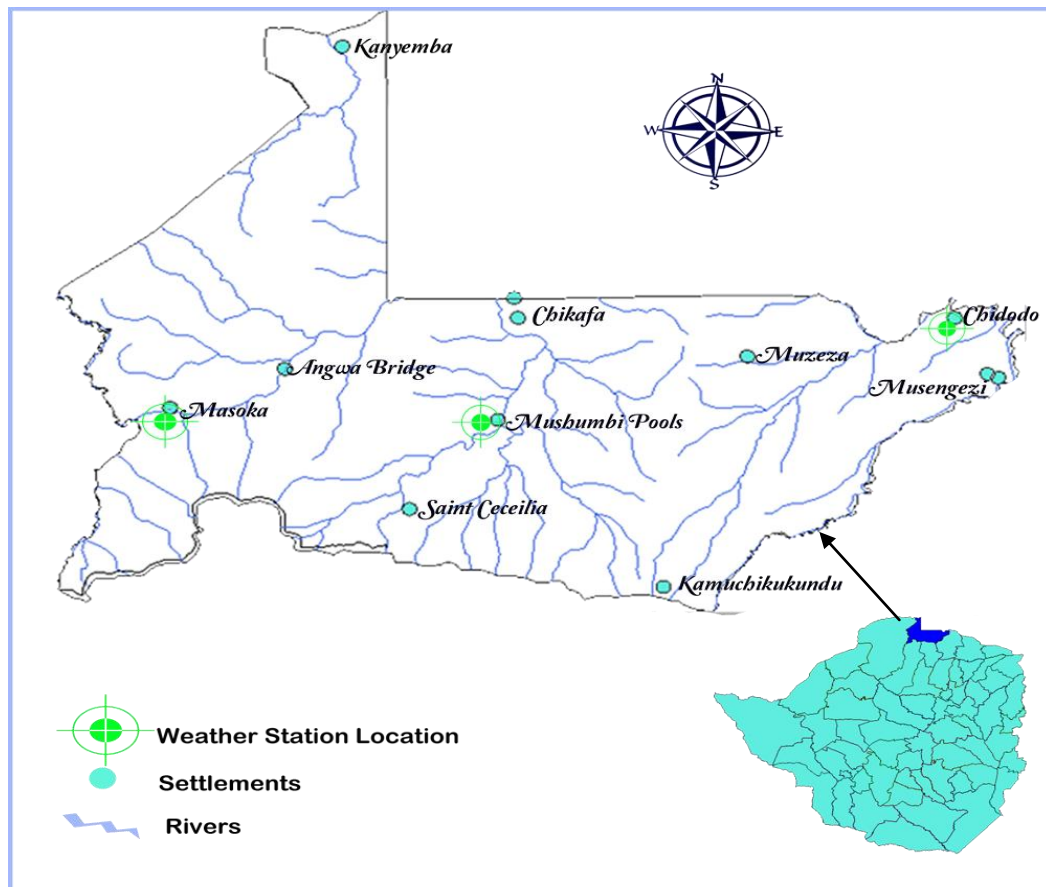


*Fig 3-1: Map of Mbire district with major settlement, weather stations and rivers*

### 3.1.1 Climate

The climate in the Mbire District is dry, with low annual rainfall of between 650-700 mm. It is variable with yearly rainfall values ranging between 550 mm and 800 mm (Phiri, 2011). The rainy season lasts for about 100 days per annum and is between November and March. The rainfall is characterized by high intensities thereby causing high soil erosion rates. The Mbire District has a mean annual temperature of 25 °C. The hottest months precede arrival of the rains. These maximum temperatures which are 40 °C and above, whereas June and July have a minimal temperatures as low as 10 °C (AWF, 2010). Figure 3-2 to Figure 3-5 shows some climatic weather variables which were measure by the automatic weather stations in the Mbire District to give an idea of the general conditions during the month of November 2015.

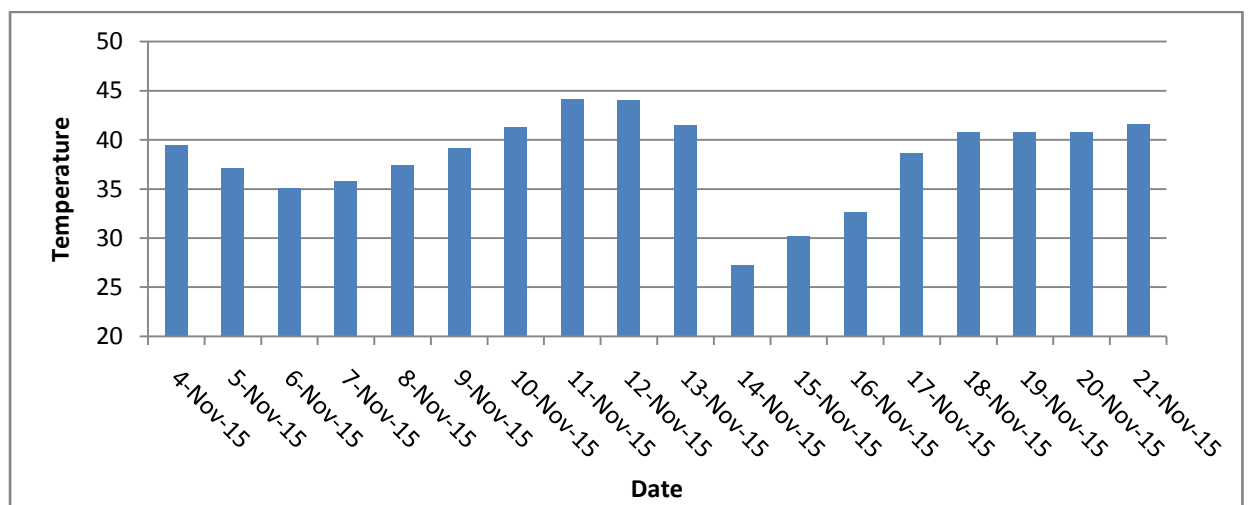


Fig 3-2: Temperature variation for November at Mushumbi, Mbire District

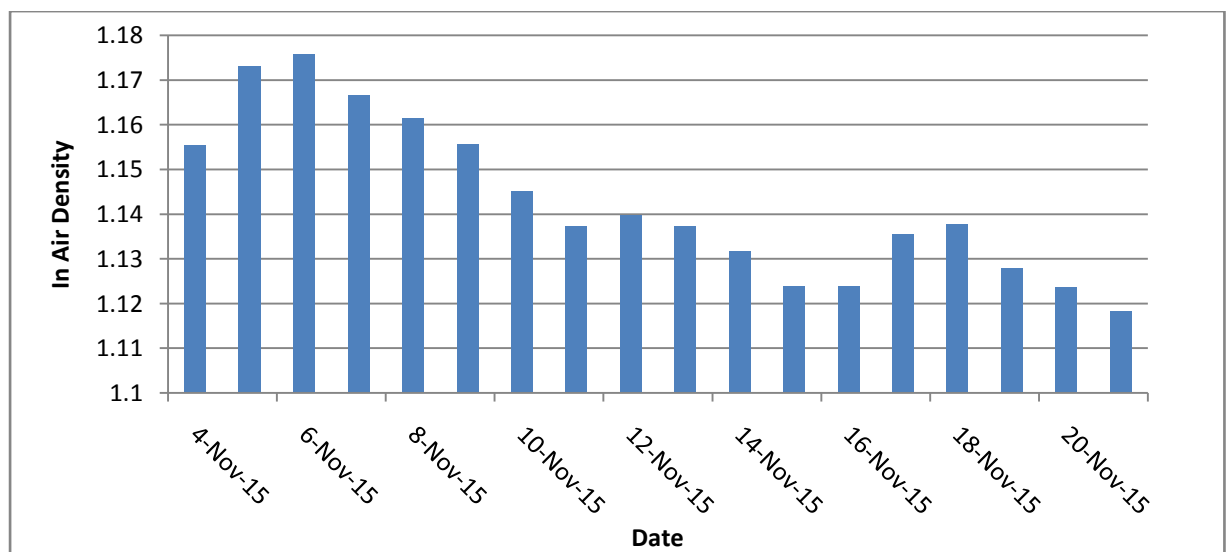


Fig 3-3: In Air Density variation for November at Mushumbi, Mbire District

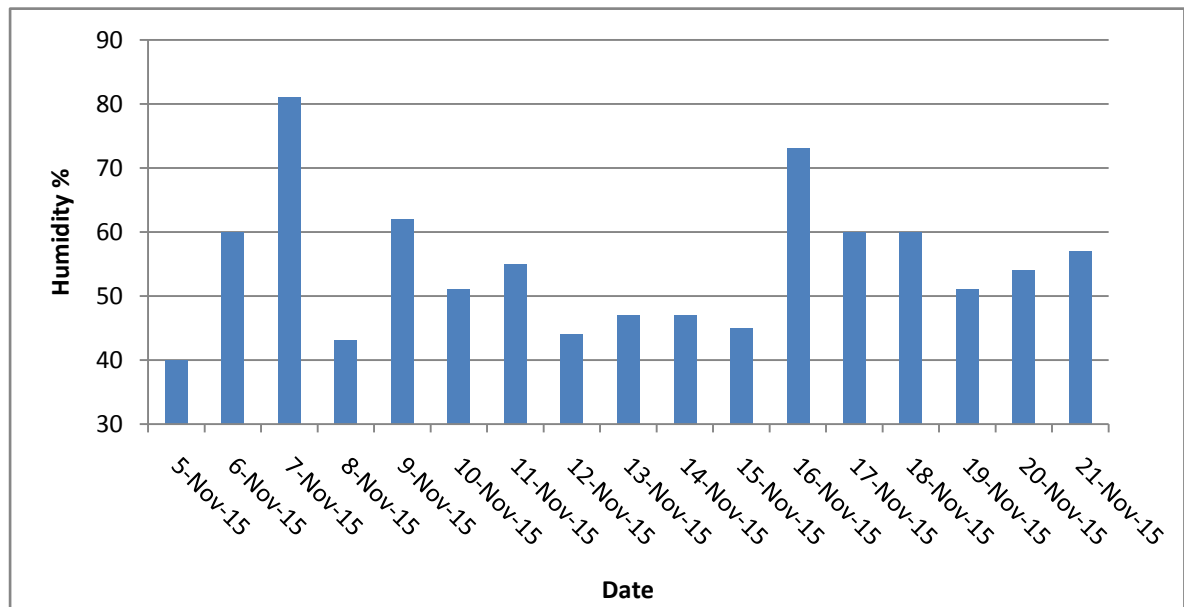


Fig 3-4: Humidity variation for November at Mushumbi, Mbire District

### 3.1.2 Soils and Geology

The Mbire District has various types of soil in the area, these include sodic calcic solonetz soils (Dube, 2011; FAO, 1996; LGDA, 2009). The majority of the Mbire District has a significant part of it having calcic solonetz soils (FAO, 1996). The most common soil type in the catchment is red soil which is acidic and easily erodible. These are some of the most common soil type: eutric cambisols, calcic, ferrall-hypoluvic arenosols and eutric leptosols. Sedimentary geological formations are the most prominent in the Mbire District with sandstone and lime foundations (CIRAD, 2001). As a result of this there is a diverse wealth of sodium and organic matter.

### 3.1.3 Livelihoods and Socio-economic issues

The economy is primarily agro-based. The majority of the communities chose to settle on watercourses (Pwiti, 1996). Historically, the population of people is extremely low because of high amount of tsetse fly which causes sleeping sickness (*trypanosomiasis*) to both animals and humans. This lasted until the 1980s, whereby a program to disinfect the area was commenced such that the area could be habitable for both humans and livestock (Kusena, 2009). The District has a total of about 116,000 inhabitants and about 21,500 households (ZimStat, 2012). These people are mainly settled along main rivers where farming is their dominant. The main activity is growing cotton, small grains and maize (AWF, 2010).

### 3.2 Research design

The research design is a combination of SEBS, TOPMODEL and meteorological data so as to conduct the water balance. The water balance is part of the assessment of water availability in the Mbire District. Remote sensing is merged with GIS and other field data in a pre field, field, and post field flow chart as shown in Figure 3-6.

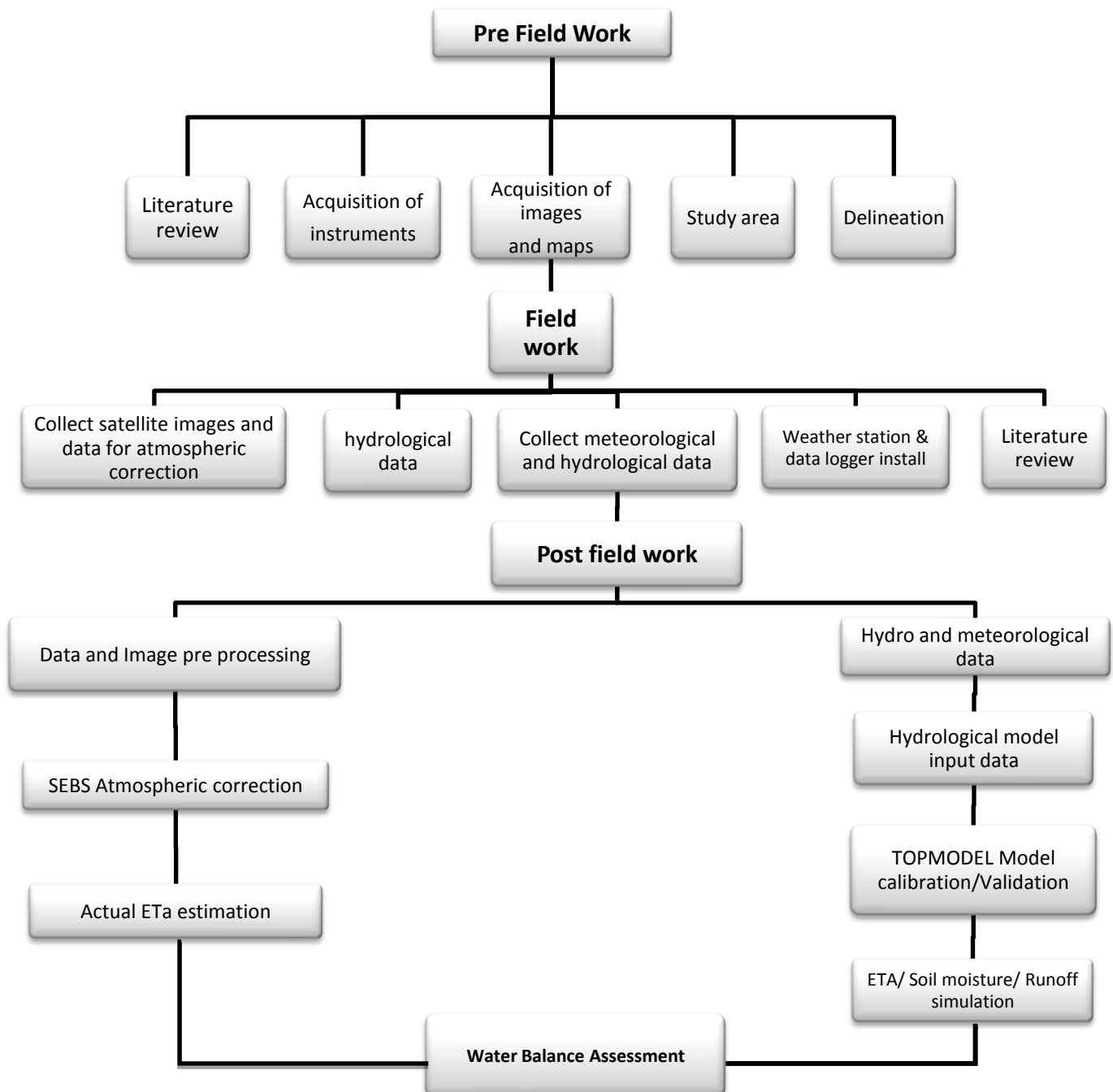


Figure 3-6: Schematic diagram showing the research process

### 3.3 Data availability and collection

Different data sets were required to determine the evapotranspiration and soil moisture. This was done by combining remote sensing, models, meteorological data and field observations from automated weather stations.

Table 3-1: Data sources and datasets used in each objective

Specific objective	Datasets used	Dataset source
1. To evaluate and compare methods of potential evapotranspiration estimation	<ul style="list-style-type: none"> <li>• Hydro meteorological data (temperature, humidity, sunshine hours, wind speed and rain fall) form 2007-2012</li> </ul>	<ul style="list-style-type: none"> <li>➤ Field observations</li> <li>➤ Meteorological Office of Zimbabwe</li> <li>➤ <a href="http://ladsweb.nascom.nasa.gov">http://ladsweb.nascom.nasa.gov</a></li> </ul>
2. To determine the spatial and temporal variation of actual evapotranspiration using the Surface Energy Balance System and the TOPODEL Concept	<ul style="list-style-type: none"> <li>• MODIS images (1km*1km), data on soil physical properties from 2005 to 2016 (October 1,2,3 images)</li> </ul>	<ul style="list-style-type: none"> <li>➤ Field observations</li> <li>➤ Meteorological Office of Zimbabwe</li> <li>➤ NASA</li> <li>➤ ZINWA and field data</li> </ul>
3. To estimate the temporal and spatial variation of soil moisture in Mbire District	<ul style="list-style-type: none"> <li>• Hydro meteorological data (temperature, humidity, sunshine , wind speed and rainfall)(October 2008-July 2013)</li> <li>• Topographic and GIS data, ASTER DEM 30m*30m resolution</li> <li>• Hydrological data (Daily water levels and discharge (October 2008-July 2013) from Angwa-Bridge, Musengezi and Manyame stations</li> </ul>	<ul style="list-style-type: none"> <li>➤ ZINWA</li> <li>➤ Meteorological office of Zimbabwe</li> </ul>
4. To Assess of Water Availability and Consumption in the Mbire District	<ul style="list-style-type: none"> <li>• Precipitation</li> <li>• River discharge</li> <li>• TOPMODEL output</li> <li>• SEBS output</li> </ul>	<ul style="list-style-type: none"> <li>➤ ZINWA</li> <li>➤ Meteorological office of Zimbabwe</li> </ul>

### **3.3.1 Meteorological data**

Meteorological data was collected from 3 automated weather stations which were installed at Chidodo clinic, Mushumbi business centre and Masoka clinic. The stations are based at 2 clinics and government offices in the case of Mushumbi.

### **3.3.2 Discharge data**

Daily discharge data for the flow gauging stations on Manyame and Musengezi River respectively were obtained. Subsequently water levels on Musengezi River were provided by the Zimbabwe National Water Authority (ZINWA). The discharge for the unknown areas was calculated as follows in Equation 26:

$$Q = \frac{1.486}{n} V R^{\frac{2}{3}} S^{\frac{1}{2}} \quad (26)$$

where;

Q	=	Discharge (m <sup>3</sup> /s)
V	=	Velocity (m/s)
N	=	Manning's coefficient
R	=	Hydraulic radius (m)
S	=	Slope of river channel (m/m)

### **3.4 Evaluation and comparison of methods of estimation of E<sub>TO</sub>**

There are many methods which have been developed to determine potential evapotranspiration; however these methods have conflicting values because of their varying assumptions and input requirements. The other reason is that they were calibrated for specific climatic areas

The FAO Penman-Monteith method was developed and selected as an alternative by which the evapotranspiration of this reference surface can be unambiguously determined, and as the method which provides consistent E<sub>TO</sub> values across all regions and climates. However, this model presents a level of input data requirement, not always available in some regions, which make its application difficult. In these cases, it is necessary to use simplified or empirical equations. These types of relationships were often subject to rigorous local calibrations and validation in order to have limited global validity. Testing the accuracy of the methods under a new set of climatic condition is frequently needed (Allen and Pereira, 1998).

To assess the performance of the five  $E_{TO}$  (Penman, Turc, Priestley-Taylor, Hargreaves-Samani and Makkink) against the FAO Penmen Monteith method, the following three criteria and assumptions are made. The first assumption is that  $E_{TO}$  should exceed  $E_{TA}$  on a long term annual basis for the forest dominated region; the second assumption is that a significant temporally stationary relationship exists between  $E_{TA}$  and  $E_{TO}$ ; and the third assumption is that the relationship between  $E_{TA}$  and  $E_{TO}$  is linear, which is necessary to assist the statistical analysis in this study. Thus,  $E_{TO}$  methods that yield the highest correlation coefficient would be the preferred ones. In practice, these assumptions are applied as  $E_{TA}$  is often estimated as a fraction of  $E_{TO}$  (Federer et al., 1996). The Pearson correlation coefficients are calculated among the methods.

$$r = \frac{n(\Sigma xy) - (\Sigma x)(\Sigma y)}{\sqrt{[n\Sigma x^2 - (\Sigma x)^2][n\Sigma y^2 - (\Sigma y)^2]}} \quad (27)$$

Table 3-2: Methods of estimating evapotranspiration

Method	Temperature	Radiation	Humidity	Others
Penman (1948) Hargreaves-Samani (1985) Priestley-Taylor (1972)	Mean Daily  Daily Maximum and Minimum Temperatures	Extra-terrestrial Radiation		
Turc (1961)	Mean Daily	Net Radiation Derived Solar Radiation and Extra-terrestrial Radiation		From Calibration Constant (1.26)
Makkink (1957) Penman Monteith	Mean Daily Mean Daily	Solar Radiation Solar Radiation	Mean Daily	

### 3.5 Evaluation of evapotranspiration using Surface Energy Balance System

#### 3.5.1 MODIS image acquisition and calibration

Level 1B calibrated MODIS radiance and reflectance satellite images were used in this study. The images ranged from the beginning of 2005 to March 2016 with more emphasis being placed on the images taken after October 2015 were validation from the newly automated weather stations had been installed into the study area.

#### *Reprojecting and converting MODIS level-1B data with ModisSwathTool*

The satellite and solarzenith and azimuth angles were ‘unpacked’ from the geolocation files through a standard operation called MODIS Swath re-projection tool (MRTSwath). MODIS bands 1–7, 31 and 32 were used. Band specific reflectance scale and offset co-efficient were retrieved from the image file using HDFview and subsequently used to convert the Level 1B simplified number to spectral reflectance and bands 31 and 32 to radiance. Band 1-7 have offsets of zero. Since bands 1 and 2 were at 250 m resolution and bands 3–7 had 500 m resolution the images were resampled to 1 km resolution so as to match spatial resolution of the radiance bands 31 and 32. The bands that were used are shown in table 3-3. The same procedure was done in the Geolocation file: *SolarZenith*, *SolarAzimuth*, *SensorAzimuth*, *SensorZenith* and Height bands were converted to GeoTIFF files (Sobrino et al., 2003).

Table 3-3: MODIS bands that were used in this research

Band	Band	Bandwidth	Primary Use
EV_250_Aggr1km_RefSB_b0	channel 1	620-670 nm	Land Boundaries
EV_250_Aggr1km_RefSB_b1	channel 2	841-876 nm	Land Boundaries
EV_500_Aggr1km_RefSB_b0	channel 3	459-479 nm	Land Properties
EV_500_Aggr1km_RefSB_b1	channel 4	545-565 nm	Land Properties
EV_500_Aggr1km_RefSB_b2	channel 5	1230-1250 nm	Land Properties
EV_500_Aggr1km_RefSB_b3	channel 6	1628-1652 nm	Land Properties
EV_500_Aggr1km_RefSB_b4	channel 7	2105-2155 nm	Land Properties
EV_1KM_Emissive_b10	channel 31	10.780-11.280 $\mu$ m	Surface Temperature
EV_1KM_Emissive_b11	channel 32	11.770-12.270 $\mu$ m	Surface Temperature

### **3.5.2 MODIS image pre-processing for SEBS**

The bands which had been converted were imported into ILWIS preprocessing using SEBS tools in ILWIS 3.7 via GDAL

#### ***Converting Raw to radiances/reflectance (MODIS)***

The images which have been imported into ILWIS are subsequently converted into radiance and reflectance. This was done in combination with the HDF file viewer which is used in the extracting of the individual reflectance's/radiances from the particular corresponding bands. The process is described in the following methods, from Equation 28 up to Equation 33.

$$\text{Reflectance} = \text{Reflectance\_scale} \quad (28)$$

$$\text{Radiance} = \text{Radiance\_scale} \quad (29)$$

$$\text{Solarzenith\_angle} = \text{solarzenith\_dn} * 0.01 \quad (30)$$

$$\text{Solarazimuth\_angle} = \text{solarazimuth\_dn} * 0.01 \quad (31)$$

$$\text{Sensorzenith\_angle} = \text{sensorzenith\_dn} * 0.01 \quad (32)$$

$$\text{Sensorazimuth\_angle} = \text{sensorazimuth\_dn} * 0.01 \quad (33)$$

#### ***Atmospheric correction of imported MODIS images***

Correction for atmospheric scattering and absorption effects on the remotely sensed reflectance signal were done using the Simplified Method for the Atmospheric Correction of Satellite data. The option is found under the SEBS pre-processing tool. Measurements were done in the Solar Spectrum (SMAC) (Rahman and Dedieu, 1994). Atmospheric correction using SMAC was done for MODIS bands 1–7. The inputs for the SMAC algorithm are: Aerosol Optical Thickness (AOT) at 0.55 $\mu\text{m}$ , water vapour content ( $\text{gcm}^{-2}$ ), ozone content (atm cm), a surface pressure map (h Pa), solar and satellite zenith and azimuth angles maps. AOT at 0.55  $\mu\text{m}$  are extrapolated from curves of wavelength specific

The reflectance was then computed using the appropriate equation (Liang, 2001).

$$\text{Albedo} = 0.16*f_1+0.291*f_2+0.243*f_3+0.116*f_4+0.112*f_5+0.018*f_7-0.0015 \quad (34)$$

where,  $f_1, f_2, f_3, f_4, f_5, f_7$  represents reflectance's which have already been corrected from MODIS's bands 1, 2, 3, 4, 5, and 7

### ***Brightness temperature computation***

The Planck equation was used in the SEBS tools to convert Band 31 and 32 to Blackbody temperatures in ILWIS which was named BTM31 and BTM32 respectively.

### ***Land surface emissivity computation***

The Land surface emissivity computation operation was used to produce the surface emissivity using the visible and near infrared bands band 1 and band 2.

Broadband albedo maps were then determined (Liang, 2001). Land surface emissivity is determined using the formulation that makes use of three NDVI classes (Sobrino et al., 2003). The three classes being bare soil ( $\text{NDVI} < 0.2$ ), mixed pixels and vegetation pixels. Land surface temperature which we named LST was determined based on the spilt window technique (Sobrino and Raissouni, 2000).

The fractional cover or proportion of vegetation (PV) map that was required for the excess resistance ( $\text{kB}^{-1}$ ) term calculation, determined as follows:

$$QV = \left( \frac{\text{NDVI} - \text{NDVI}_{\min}}{\text{NDVI}_{\max} - \text{NDVI}_{\min}} \right)^2 \quad (35)$$

Roughness makes use of the Leaf Area Index (Gowda et al.), calculated from NDVI. Leaf Area Index (LAI) is calculated internally in the SEBS algorithm using the following equation:

$$\text{LAI} = \left[ \text{NDVI} \left( \frac{1 + \text{NDVI}}{1 - \text{NDVI}} \right) \right] 0.5 \quad (36)$$

### ***Land surface temperature computation***

The land surface temperature was calculated according to an equation by Sobrino, (2003)

$$LST = band31 + 1.02 + 1.79 * (band31 - band32) + 1.2 * (band31 - band32)^2 + (34.83 - 0.68 * l) * (1 - e) + (-73.27 - 5.19 * l) * se \quad (37)$$

where;

<i>LST</i>	=	Temperature (K)
<i>band31</i>	=	Brightness temperature band 31 (K)
<i>band32</i>	=	Brightness temperature band32 (K)
<i>l</i>	=	Water vapor content (g.cm <sup>-2</sup> )
<i>E</i>	=	Surface emissivity
<i>se</i>	=	Surface emissivity difference

### ***Meteorological data***

The meteorological variables used in running SEBS algorithm were as follows, air temperature (°C), specific humidity [kg/kg], wind speed (ms<sup>-1</sup>), solar radiation [W m<sup>-2</sup>] and pressure at the surface and reference height (Pa). Solar radiation can be determined from the automated weather stations

## **3.6 Estimating the spatial and temporal variation of soil moisture and E<sub>TA</sub> using TOPMODEL**

TOPMODEL results can be manipulated so as to determine variation of soil moisture using the wetness index to average storage deficit (Moges, 2008). The model was calibrated for runoff simulation before soil moisture was determined. This is because the stream-flow output from the TOPMODEL parameters (transmissivity, base flow, wetness index and local storage deficit) in combination with meteorological data are used in the ILWIS command line for soil moisture simulation.

### 3.6.1 TOPMODEL parameters

Table 3-4 outlines the range of values for the different parameters used in TOPMODEL simulation. The values are found in a text file known as the “param” file. It is consistently updated and edited in the calibration process.

Table 3-4: Parameter values used and their definitions

Parameter	Description	Unit	Range of values
M	A parameter which controls the rate of exponential decrease of transmissivity with increasing soil moisture	[m]	3-6
Ln(T <sub>0</sub> )	The natural logarithm of transmissivity at saturation in the parameter file	[m <sup>2</sup> /hr]	3-6
TD	Time delay constant in the parameter file	[-]	18-25
CHV	The effective surface routing velocity	[m/hr]	3500 - 4100
RV	The stream velocity	[m/h]	-
SRMAX	Maximum root zone storage deficit	[m]	-
Q <sub>0</sub>	Initial base flow	[m]	-
SR <sub>0</sub>	Root zone storage at start	[m]	-

### 3.6.2 DEM hydro processing

An ASTER DEM (30m resolution) covering the Mbire District study areawas retrieved from <http://www.gdem.aster.ersdac.or.jp/>.

#### *Removal/filling of sinks*

The operation used to fill sinks in ILWIS removed local depressions. The height values of a local depression consisting of multiple pixels were raised to the lowest value of a pixel adjacent to the outlet for the depression and that would discharge into the preliminary depression (Hengl et al., 2007). This ensured that flow direction was found for every pixel in the map.

### ***Flow determination***

Flow direction was computed using the D8 algorithm in ILWIS software which could take eight different directional value stated in degrees and numeric codes. The D8 method can be used more effectively in drainage networks with channels that are highly developed (Garbrecht and Martz, 1999).

### ***Network and catchment extraction***

The algorithm in ILWIS was used extract drainage network from the filled Mbire DEM, flow direction and flow accumulation. The drainage network was ordered and the desired catchments were extracted from which three desired catchments for Mbire district were extracted based on the location of upstream gauging stations. These catchments are Manyame, Musengezi and Angwa.

### **3.6.3 TOPMODEL inputs**

The catchment was subdivided into three and the wetness index was calculated for each. An ASTER DEM of (30\* 30) resolution was used in ILWIS 3.3 Academic (ITC, 2007).

$$TI = \ln(A/\tan B) \quad (38)$$

where;

$$\begin{aligned} \tan B &= \tan [\text{DEGRAD}(\text{SLOPEDEG})] \\ A &= \text{Flow Accumulation} * 900 \\ \text{SLOPEDEG} &= \text{RADDEG} [\text{ATAN}(\text{SLOPEPCT}/100)] \\ \text{SLOPEPCT} &= 100 * \text{HYP}(DX, DY) / 30 \text{slope} (\%) \end{aligned}$$

### ***Potential evapotranspiration calculation***

For daily estimate of potential evapotranspiration the Food and Agricultural Organization (FAO) uses Penman-Monteith method (Allen and Pereira, 1998) as described in Equation 1.

### ***Discharge calculation***

To determine discharge, the Manning's Equation was used. This was so as to account for discharge where ZINWA had not been able to measure. The Manning's Equation estimates velocities and flow rates given a measure of the physical characteristics of a stream

$$Q = \frac{1.486}{n} R^{2/3} S^{1/2} \quad (39)$$

where;

Q	=	Discharge (m <sup>3</sup> /s)
V	=	Velocity (m/s)
N	=	Manning's coefficient
R	=	Hydraulic radius (m)
S	=	Slope (m/m)

### 3.6.4 TOPMODEL calibration

The model was calibrated based on three parameters using knowledge obtained from the following (Beven, 1997; Beven and Freer, 2000; Beven et al., 1995; Beven, 2001; Beven and Kirkby, 1979; Gumindoga, 2010; Muhammed and Enschede, 2012) known to be the most sensitive. An average root zone available water capacity (SRmax) can be used for each sub-catchment. A time step of 24 hour is selected for computations to calibrate the model. The value of parameter 'm' is varied, holding values of remaining four parameters at initial value and value of parameter 'm' is determined to find the highest efficiency. This method is repeated for the remaining parameters to arrive at a set of parameters, which give the highest value of efficiency. The main indicator of good performance is Nash-Sutcliffe's coefficient of efficiency (NSE)

$$NSE = \frac{\sum_{i=1}^n (S_i - O_i)^2}{\sum_{i=1}^n (O_i - \hat{O})^2} \quad (40)$$

$S_i$	=	Simulated value
$O_i$	=	Observed value
$\hat{O}$	=	Average observed value

### 3.6.5 TOPMODEL validation

The model was validated using a selected dataset. The simulated stream flows then compared to observed stream flow, graphically and numerically using certain particular performance indicators. Nash-Sutcliffe Efficiency (NSE) (Nash and Sutcliffe, 1970) is used as a performance indicator in this study are the percent bias (PBIAS). Percentage difference of runoff (PDQ) was calculated as follows:

$$PDQ = \frac{(S_i - O_i) * 100}{O_i} \quad (41)$$

$$L_t = t_t^S - t_i^O$$

where;

$S_i$	=	Value simulated
$O_i$	=	Value observed
$t_t^S$	=	Simulated occurrence time
$t_i^O$	=	Simulated observed time

### 3.6.6 Soil moisture estimation using TOPMODEL

This computation is done in the ILWIS command line and post validation of TOPMODEL. The value of soil moisture (D) comes from calculating the mean of  $S\_bar$  values which is the initial storage deficit. The scaling parameter comes from the parameter file used in running the model. The  $TanB$  and  $WI$  maps are all inputs from hydro processing. The spatial variation of soil moisture ( $SM_i$ ) was derived from the Equation 36 (Moges, 2008).

$$SM_i = S\_bar - m[TI - Ln \frac{A_i}{T_0 tan B_i}] \quad (36)$$

where;

$S\_bar$	=	Initial storage deficit
$WI$	=	Wetness Index map
$m$	=	Scaling parameter
$T_0$	=	Transmissivity at saturation
$A_i$	=	Area of catchment
$TanB_i$	=	Tangent of slope map

In order to compare the soil moisture with ground based data a soil moisture logger was used. The HOBO data logger has a 12-bit resolution. It can record up to 43,000 events or measurements. The four external channels accept a wide range of Onset and third-party sensors/transducers with a 0-2.5 VDC output, including temperature, AC current, air velocity, pressure and sensors.

The logger was installed in Chidodo area which is in the Musengezi sub-catchment at coordinates, 16.0154° south, 31.1128° east and at an elevation of 326 m above sea level. The logger has three depth levels of installation in the ground; these are 150 mm, 300 mm and 750 mm below the surface. TOPMODEL simulated soil moisture is compared with the probe placed 150 mm below

the surface because it is at the same level as the temperature probe. The logger does not measure soil moisture directly but rather measures voltage which has to be converted to volumetric moisture content. To be able to compare this to the soil moisture from TOPMODEL the volumetric soil moisture is then converted to a percentage of the maximum moisture and so is the TOPMODEL soil moisture. The TOPMODEL soil moisture is taken precisely from the pixel which coincides with the logger coordinates. The two are then compared as percentages of the maximum soil moisture.

### **3.7 Assessment of Water Availability and Consumption in the Mbire District**

Using precipitation values from the automated weather stations stationed at Masoka, Chidodo and Mushumbi from November 2015 to February 2016, discharge accounted for by the TOPMODEL rainfall runoff model,  $E_{TA}$  derived from both TOPMODEL and SEBS algorithm, Equation (37) was used to conduct a water balance so as to assess the availability in the Mbire District. The water balance was computed for the 3 sub-catchments which Angwa, Manyame and Musengezi.

These values were converted into volumes by multiplication with sub-basin areas to allow volumetric assessments.

$$S = P + Q_{in} + G_{in} - E_{TA} - Q_{out} \quad (37)$$

where;

$P$	=	Precipitation
$Q_{in}$	=	Surface water inflow
$G_{in}$	=	Groundwater inflow
$E_{TA}$	=	Actual evapotranspiration
$Q_{out}$	=	Surface water outflow
$G_{out}$	=	Groundwater outflow
$S$	=	Storage change during the time interval

## **4. RESULTS AND DISCUSSION**

The data from the automated weather stations was used to determine the most accurate method to determine potential evapotranspiration. Secondly the evapotranspiration results obtained from the RS methods are analysed and later compared with the automated weather station data. Thirdly, TOPMODEL soil moisture simulations are compared with the soil moisture from the hobo data logger data loggers. Finally the outputs of the SEBS, TOPMODEL and Meteorological data are put together to analyze the water balance in the District.

### **4.1 Evaluation and comparison of point based methods of estimation of potential $E_{TO}$**

The analysis evaluation was conducted for a total of 2191 daily observations carried out from 2007 to 2012. Table 4-1 shows the results for this comparison, using simple statistical regression analysis, indicating error estimation and index of agreement.

The Makkink and Penman methods achieved the best performances, with higher coefficients of determination (over 0.7) and indices of agreement being 0.80 and 0.43. They present RMSE lower than  $1 \text{ mm.day}^{-1}$ , which corresponds to a relative error under 20 %. After Priestley-Taylor and Penman methods, Hargreaves, Turc and Makkink approaches presented better behaviour. They presented RMSE values close to  $1 \text{ mm.day}^{-1}$ , with relative errors around 25 % respectively. The Penman equation presented the highest RMSE (equal to  $0.93 \text{ mm.day}^{-1}$ ) with a relative error over 25 % and an index of agreement equal to 0.43

Table 4-1: Evaluation of the various methods for calculating mean daily ETp

METHODS	$P_{avg}$	$P_{avg}/O_{avg}$	$E_{t0}(\text{FAO056 Penman Monteith}) = A + B(E_{t0})$			RMSE	relRMSE	d
	mm/day	%	A	B	$R^2$	mm/d	%	
Hargreaves	4.79	131	2.10	0.7378	0.6087	1.22079	33.3	0.11886
Priestley_Taylor	2.72	74.3	0.0536	0.7297	0.9011	0.968183	26.4	0.372675
Makkink	4.77	130	0.4478	1.183	0.7676	1.211019	33.1	0.802054
Turc	1.71	46.6	- 0.3008	0.5488	0.8226	1.98356	54.2	-0.5744
Penman	2.74	75.0	- 0.6403	0.9254	0.9327	0.930198	25.4	0.431942

Regression analysis of the values calculated by various methods over those calculated by FAO56-Penman-Monteith. Number of observations: 4026;  $P_{avg}$ : mean of the values calculated by various methods;  $O_{avg}$ : mean of the values calculated by FAO56-Penman-Monteith (3.66 mm.day<sup>-1</sup>); A: ordinate at the origin; B: slope regression coefficient;  $R_2$ : coefficient of determination; RMSE: root mean squared error; RelRMSE: relative error; d: index of agreement.

With respect to over/under estimation of FAO56-Penman-Monteith equation, there were significant over estimations from Hargreaves and Makkink of approximately 30 % each. On the other hand, there were significant under estimations by Priestley Taylor, Turc and Penman. Turc produced the most significant underestimation with a value of 46.6 %. Figures 4-1 to 4-5 shows the relationship between FAO Penman Monteith and the respective empirical equation. Figure 4-1 shows the relationship between Penman Monteith and Hargreaves with coefficient of determination of 0.6. This is a relatively low compared to the other  $R^2$  values which is contrary to other studies which concluded that Hargreaves was the best in that particular area. It has been successfully used in other regions to determine  $E_{TA}$  (Shahidian. S. et al., 2003). Figure 4-2 up to 4-5 shows the Turc, Priestly Taylor, Makkink and Penman relationships with a high  $R^2$  values of 0.82, 0.9, 0.7, and 0.93 respectively. This high value results were consistent with another study Central Serbia (Alexandris et al., 2008).

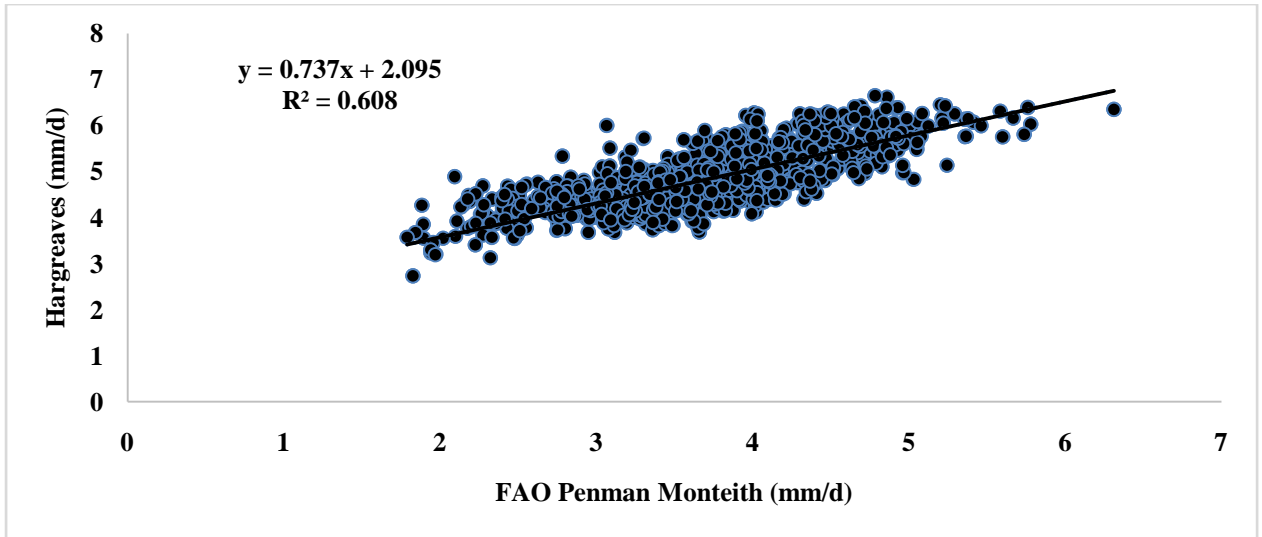


Fig 4-1: The relationship between E<sub>Tp</sub> of Penman Monteith and Hargreaves equation

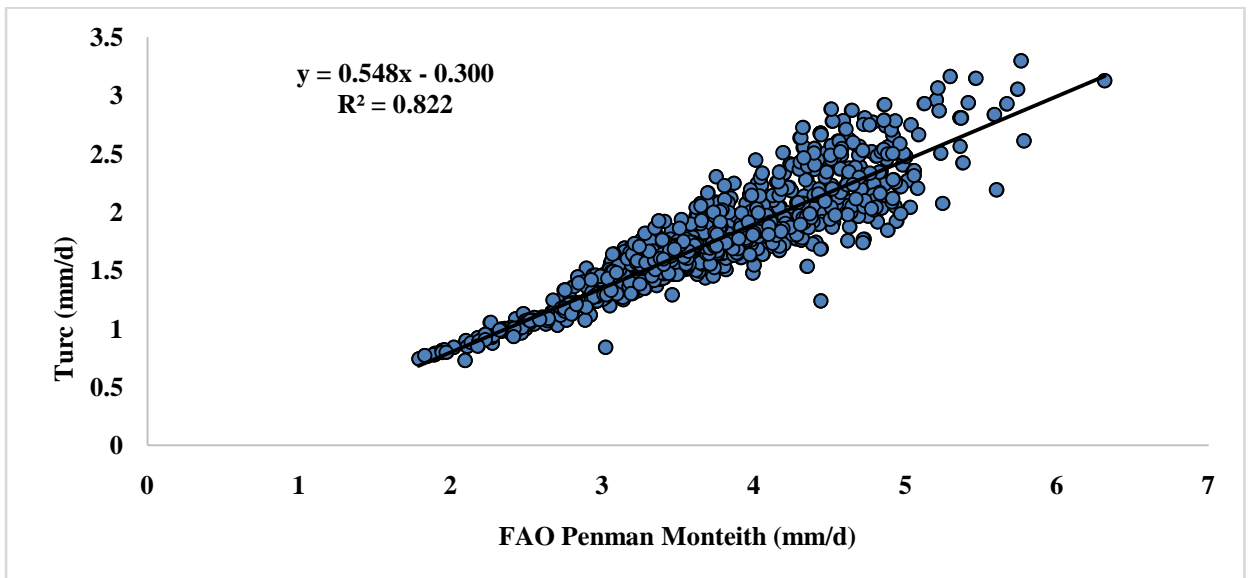


Fig 4-2: The relationship between E<sub>Tp</sub> of Penman Monteith and Turc equation

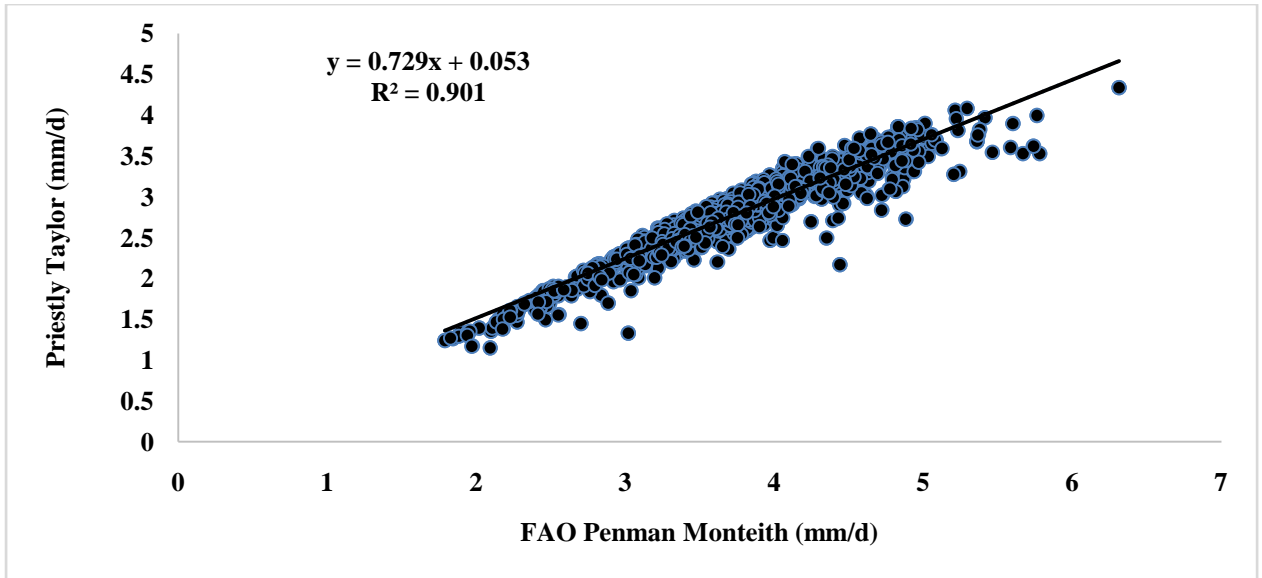


Fig 4-3: The relationship between ET<sub>p</sub> of Penman Monteith and Priestley-Taylor equation

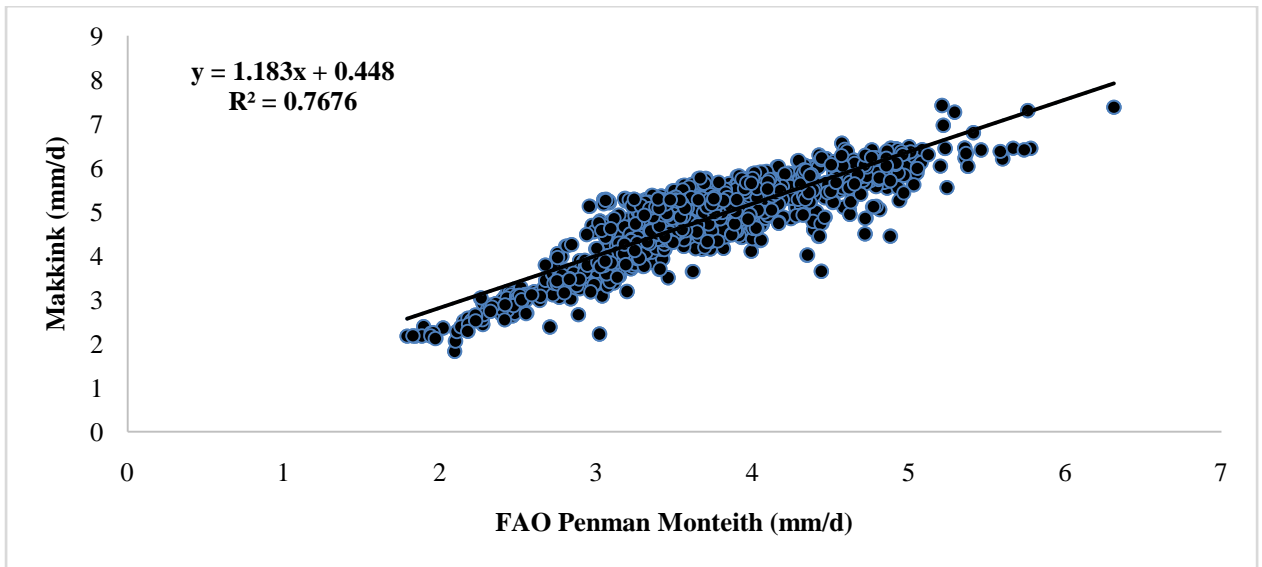


Fig 4-4: The relationship between ET<sub>p</sub> of Penman Monteith and Makkink equation

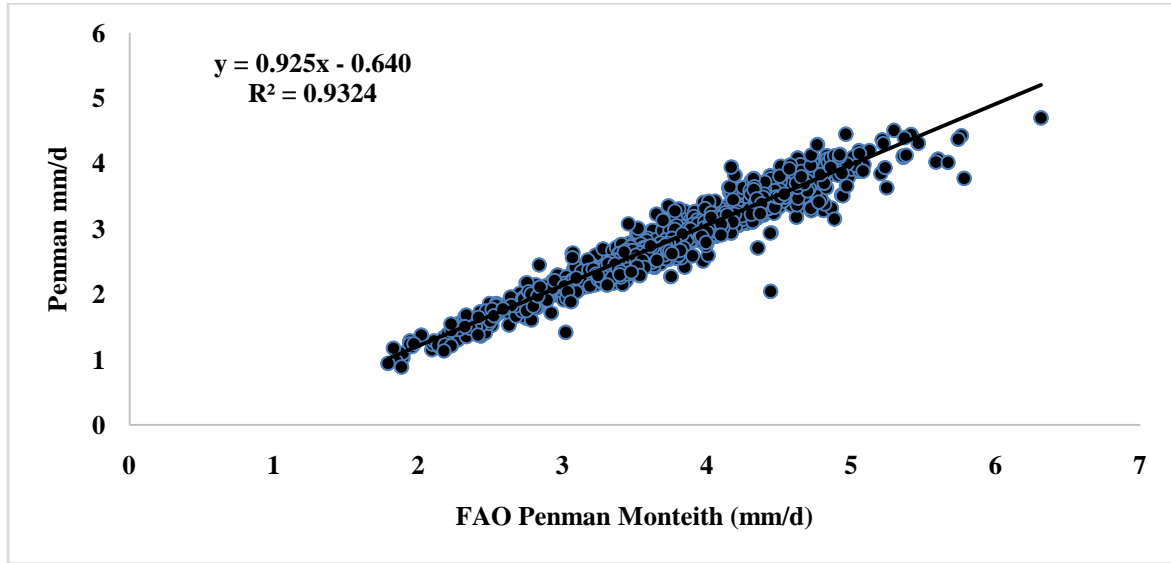


Fig 4-5: The relationship between  $E_{Tp}$  of Penman Monteith and Penman equation

#### 4.2 The spatial and temporal variation of $E_{TA}$ in the Mbire District

The SEBS algorithm was successful in retrieving actual evapotranspiration. A single image was taken between the 1<sup>st</sup> and 2<sup>nd</sup> of August every year from 2005 to 2015. Table 4-2 presents  $E_{TA}$  from 2005-2015 in the month of August. The graph corresponding to this table is then shown in Figure 4-6 with a generally increasing trend of  $E_{TA}$ . The Maximum and minimum values for  $E_{TA}$  were 6.13 mm/day and 3.30 mm/day respectively. Figure 4-8 shows  $E_{TA}$  values from 2007-2014. The trend in the graph shows as general increase in  $E_{TA}$ . This may be due to an increase in temperature of the past 10 years, as well as changes in land use, i.e. the increase in deforestation and clearing of land for agricultural purposes (Rwasoka et al., 2011).

Table 4-2: The mean  $E_{TA}$  from 2005 to 2015 for the Mbire District

Year	2005	2006	2007	2008	2009	2010	2011	2012	2013	2014	2015	Mean	Max	Min
Eta (mm/day)	4.44	3.30	6.13	4.79	5.54	5.20	5.33	5.03	5.73	5.11	5.69	5.12	6.13	3.30

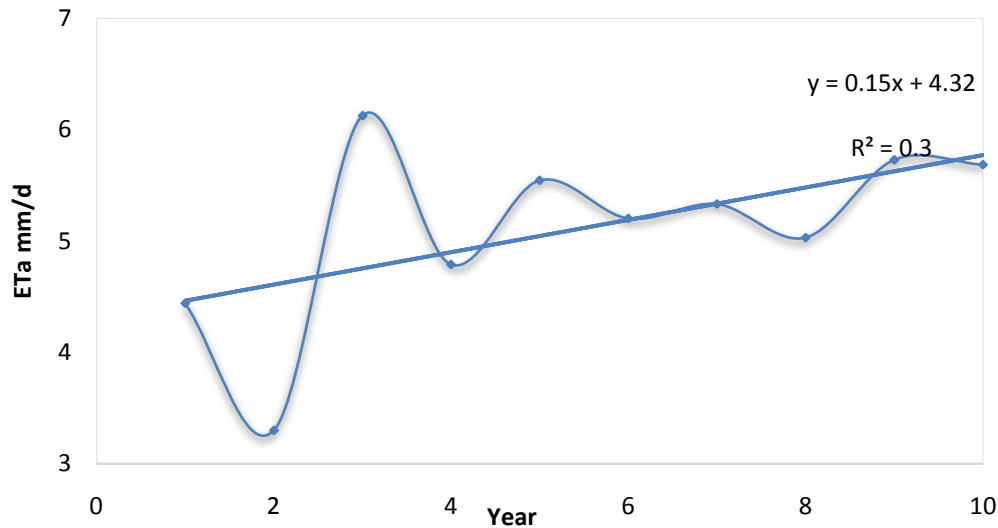


Fig 4-6: The variation of  $E_{TA}$  from 2005 to 2015 in the month of August

More images were taken within the study period (November to March). This was done within the time which the automated weather stations were setup in the Mbire District. The corresponding TOPMODEL driven  $E_{TA}$  is shown in Figure 4-7. Three images were taken every month from November to March. The graph showing these results is shown in Figure 4-7 and the details are shown in Table 4-3. The average  $E_{TA}$  is 4.11 mm/day for TOPMODEL and 3.61 mm/day for SEBS. TOPMODEL estimates values which are much generally higher than SEBS. This could be as a result of varying scaling parameters used in calibrating TOPMODEL. This allowed for comparison between the  $E_{TA}$  retrieved by the SEBS and the  $E_{TA}$  calculated from the TOPMODEL. High values of relative evapotranspiration were found in densely forested (6 mm/day) as compared to grassland (3 mm/day) regions. This may be due to the high availability of moisture from the dense vegetation. A similar study done by Rwasoka showed varying  $E_{TA}$  depending on the land cover (Rwasoka et al., 2011).

Table 4-3: The mean  $E_{TA}$  from October 2015 to February 2016

Date	Nov	Nov	Nov	Dec	Dec	Dec	Jan	Jan	Jan	Feb	Feb	Feb	Mar	Mar	Mar	Mean	Max	Min
SEBS $E_{TA}$ (mm/day)	3.12	3.52	3.21	4.0	2.87	4.20	4.63	6.04	2.54	3.44	4.11	3.22	2.54	4.01	2.65	3.61	6.04	2.54
TOPMODEL $E_{TA}$ (mm/day)	4.42	4.62	4.15	3.93	4.21	3.41	3.8	4.06	4.61	3.5	4.82	4.8	4.86	3.4	3.12	4.114	4.86	3.4

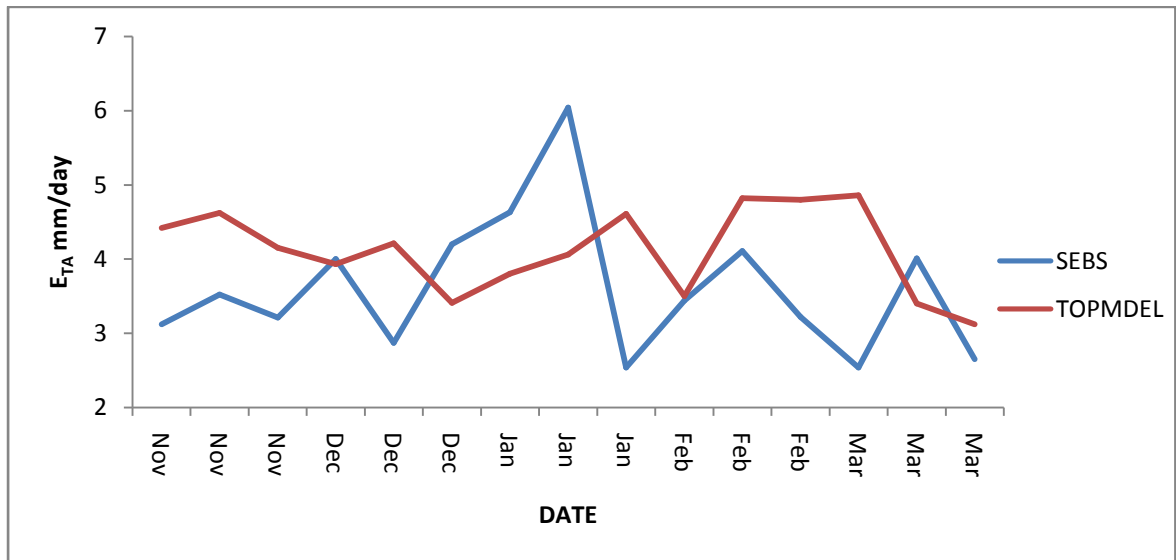


Fig 4-7:  $E_{TA}$  of the Mbire District in Nov 2015-Mar 2016

The variation of  $E_{TA}$  in the 3 months shown in Figure 4.7 was such that there was a peak in January of 6 mm/day. This may have been due to the increase in availability of moisture on the soil surface as a result of the rainfall which was increasing from the month of November onwards. It is also worth mentioning that the MODIS images are taken in the morning hour (9 am) of the day when temperatures are generally depressed. This suggests that the peak  $E_{TA}$  of the 24 hr day is not captured and can only be inferred.

The actual evapotranspiration simulated by TOPMODEL depicts a constant value of 5mm/day from the middle of February to early March. This may be a result of incorrect estimations in the rainfall data obtained from ZINWA. However, 5 mm/day may very well be the maximum value that can be achieved from the parameter settings.

A remote sensing based approach to determine the water balance for the Mbire District of Zimbabwe

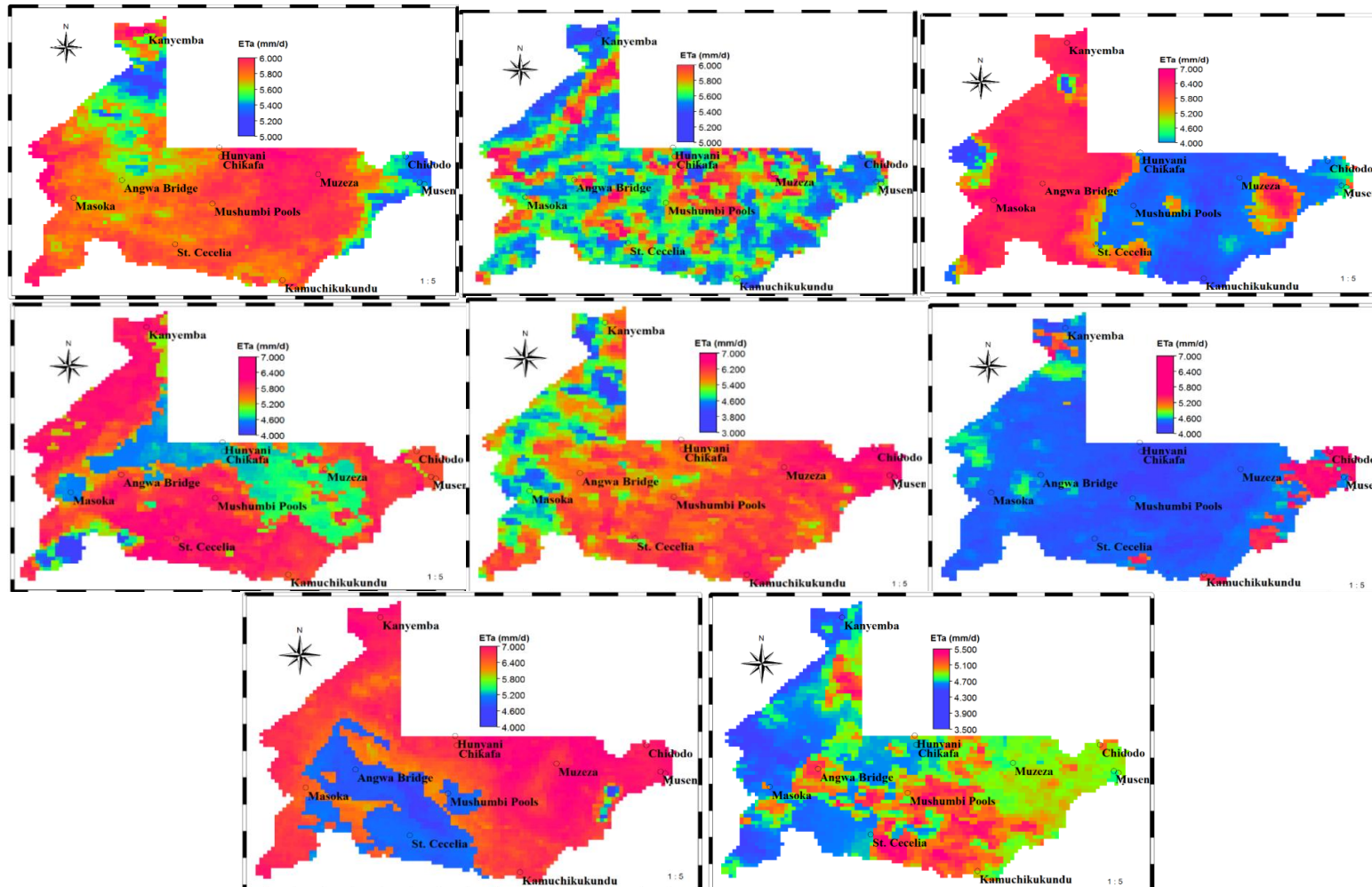


Fig 4-8:  $E_{TA}$  of the Mbire District in October from 2007- 2014

SEBS based actual evapotranspiration was compared with TOPMODEL based  $E_{TA}$ . The two were then checked against potential evapotranspiration to establish whether the  $E_{TA}$  values were in fact, less than  $E_{TO}$  generally. After the calibration and validation of TOPMODEL actual evapotranspiration was determined by extracting values of potential evapotranspiration from the TOPMODEL results and using the values in Equation 28. The results showed that potential  $E_{TO}$  was greater than  $E_{TA}$  for both SEBS and TOPMODEL on the 1<sup>st</sup> of August 2008 and 2009. This result is consistent with the theory that  $E_{TO}$  should always be greater than  $E_{TA}$  under steady state conditions (McMahon et al., 2013). The results are presented in Table 4-4.

Table 4-4: Actual evapotranspiration results comparing SEBS/TOPMODEL to  $E_{TO}$

Evapotranspiration Method	SEBS mm/day	TOPMODEL mm/day	Potential ET mm/day
1 August 2008	4.789	4.986	5.54
1 August 2009	5.545	4.927	5.65

### 4.3 Estimation of the spatial and temporal variation of soil moisture using TOPMODEL

#### 4.3.1. Spatial variation of terrain input

Fig: 4-9 to 4-11 illustrates sub catchments inputs used in DEM hydro processing. These are filled DEM, flow direction and flow accumulation, they are shown for Manyame, Musengezi and Angwa River sub catchment as computed from DEM hydro processing.

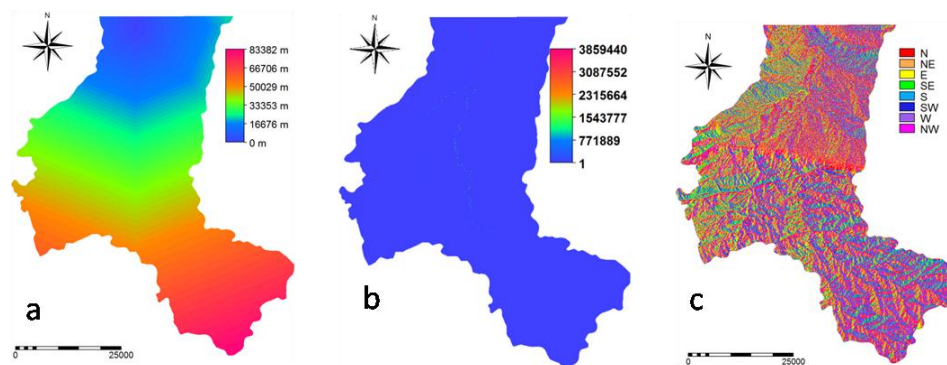


Fig 4-9: Hydro-processing (a) distance map (b) flow accumulation (c) flow direction for Manyame

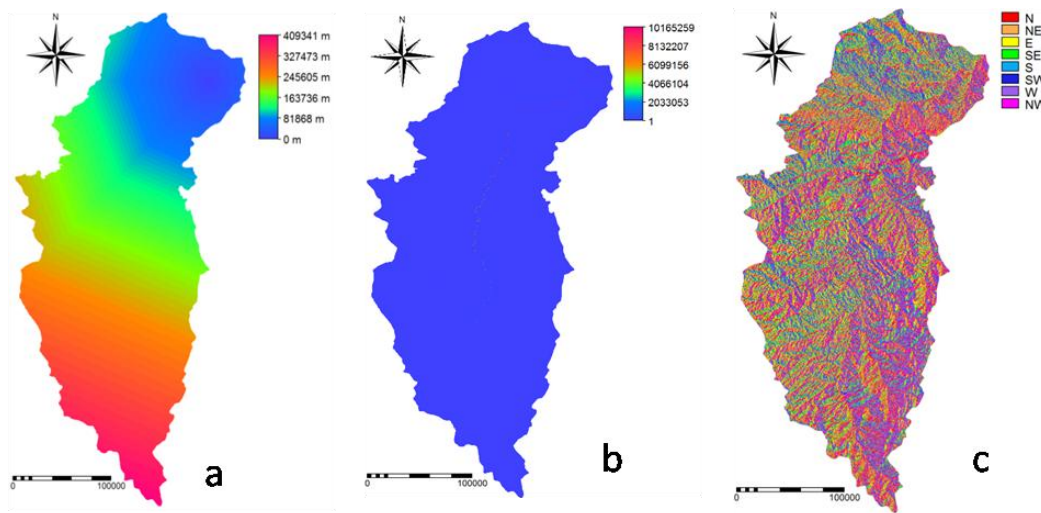


Fig 4-10: Hydro-processing (a) distance map(b) flow accumulation (c) flow direction for Angwa

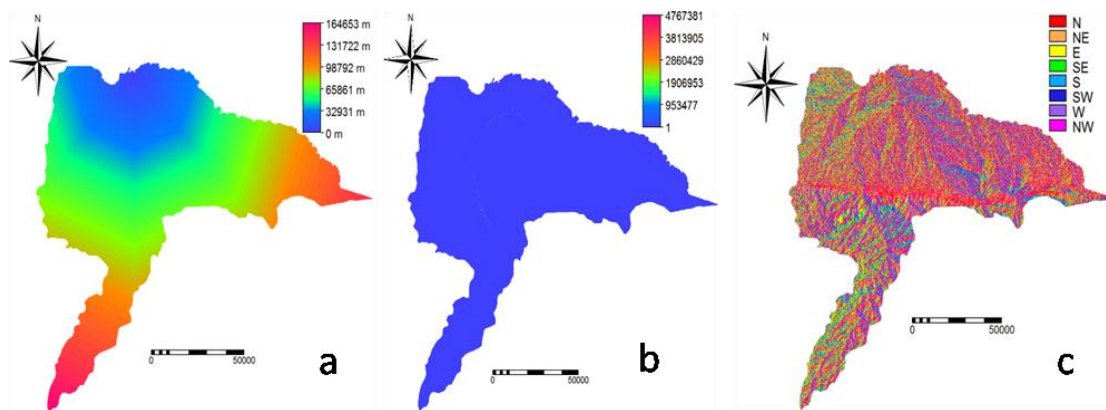
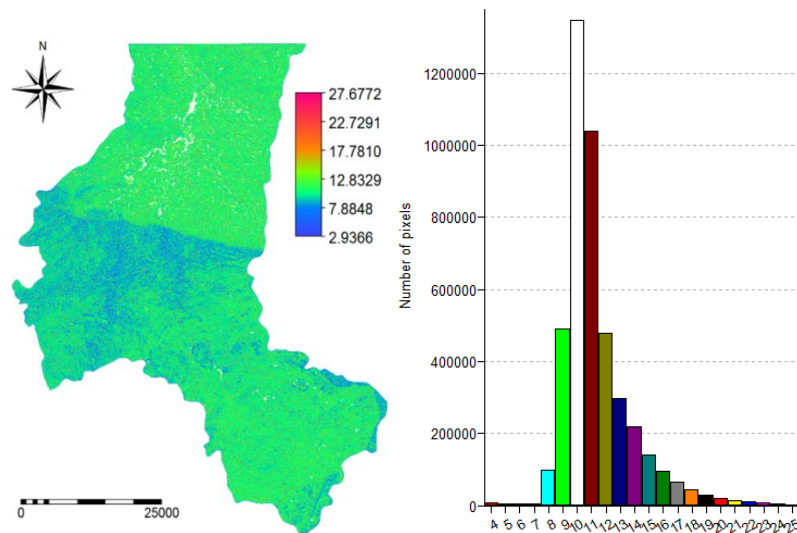


Fig 4-11: Hydro-processing (a) distance map (b) flow accumulation (c) flow direction for Musengezi

### 4.3.2 The spatial variation of the Wetness Index

Higher wetness indices are found in the northern part of the basin in and around the Manyame River. The highest number of pixels is found in the region of 10 followed by 11. The lower the  $Tan\beta$  values, the lower the hydraulic gradient and subsequently there is more accumulation of water. In similar fashion the higher  $\ln(a/tan\beta)$  implies a higher degree of wetness thus more soil moisture which is being contributed by higher sloping areas. This maintains the TOPMODEL's theory and principal that areas with low surface gradients and big contributing areas have higher soil moisture than those areas which have small contributing areas (Band *et al.*, 1991). An example of a Wetness index Map for Manyame is shown on Fig 4-12.



*Fig 4-12: Wetness Index histogram and map for Musengezi River sub-catchment*

### **4.3.3 Runoff calibration results for Manyame and Angwa River sub catchments**

There was 4 years of data available for both validation and calibration. The data was then divided into two, each process being allocated 2 years each. Calibration was from 01 October 2008 to 31 August 2010. The Nash-Sutcliffe coefficient of efficiency (NSE) was average for Manyame and below average for Angwa (NSE= 0.35 and 0.1 for Manyame river and Angwa river sub catchments respectively) while the percent bias (PBIAS) (PBIAS= -9.54 and -6.03% for Manyame river and Angwa river sub catchments respectively). Validation was from 1 September 2010 to 31 July 2013. The optimized model parameter obtained from final validation and together with corresponding Nash-Sutcliffe's (NSE) value as well as the percent bias (PBIAS) for the three sub-catchments, Manyame, Musengezi and Angwa River are illustrated in Table 4-5.

Table 4-5: Model parameters and model efficiency after validation

<b>Sub catchment</b>	<b>Parameter</b>	<b>Optimized</b>	<b>NSE</b>	<b>PBIAS (%)</b>
<b>Musengezi</b>	SRmax (m)	0.0480	0.1	0.003
	m	3.5		
	T0 (m <sup>2</sup> /s)	0.040		
<b>Manyame River sub catchment</b>	SRmax (m)	0.0560	0.35	0.0012
	m	3		
	T0 (m <sup>2</sup> /s)	0.075		
<b>Angwa River sub catchment</b>	SRmax (m)	0.030	0.15	0.035
	m	3.4		
	T <sub>0</sub> (m <sup>2</sup> /s)	0.052		

Figure 4-13 shows a comparison between simulated and observed runoff for Manyame. There is an evident mis-simulation of discharge on 5 January 2009. This may be a result of the parameters used in the calibration of the model being slightly wayward and thus needing more tempering.

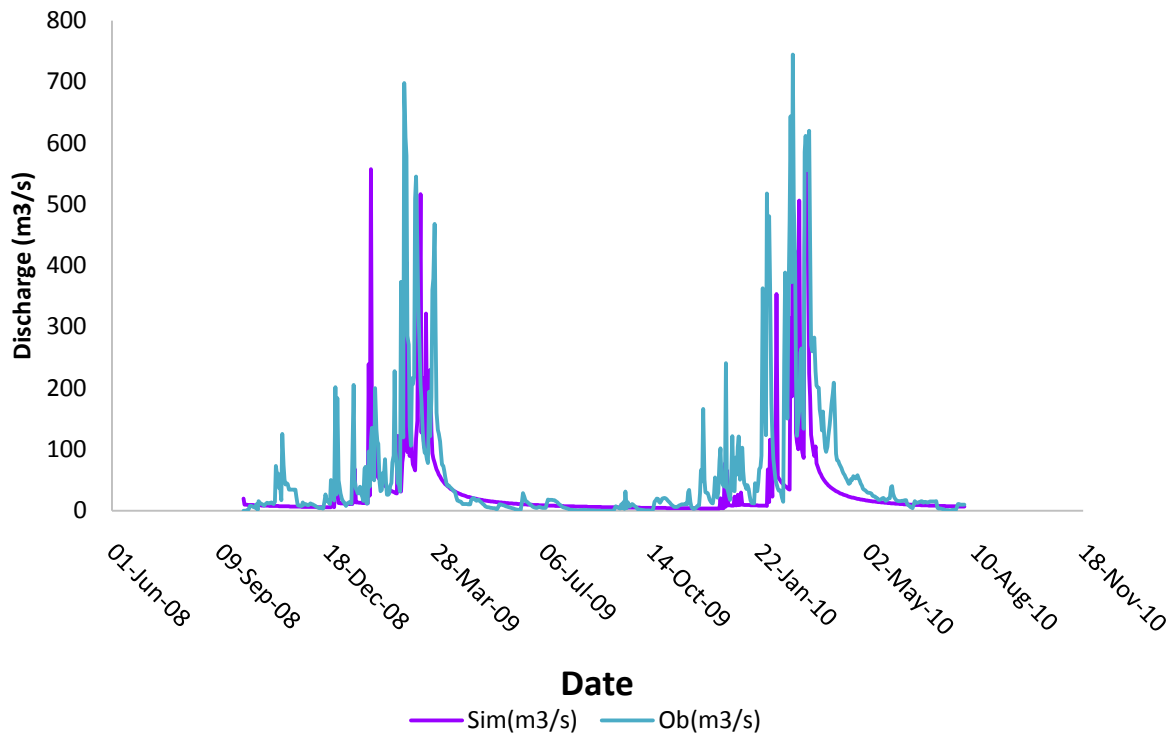
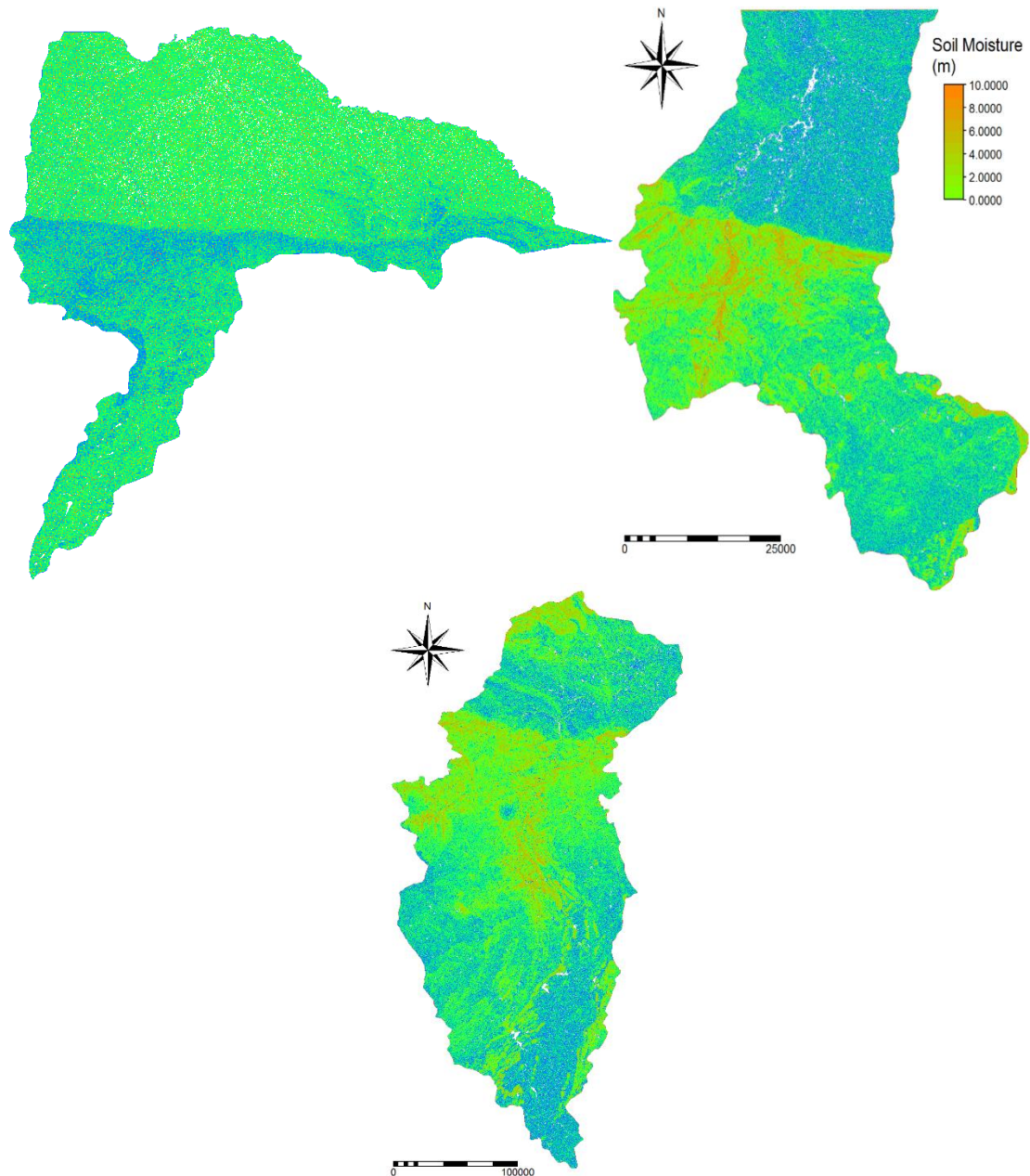


Fig 4-13: Comparison between simulated and observed runoff for Manyame sub catchment

#### 4.3.4 The spatial variation of soil moisture using TOPMODEL

TOPMODEL was calibrated and validated so as to determine the variation of soil moisture and thereafter, comparing the results with those of the automated soil moisture data logger. The Musengezi River sub catchment was unfortunately not in relevant agreement with the observed discharge for Musengezi River sub catchment, therefore no comparison could be made using the sub catchment. This could be due to the fact that levels from gauging station C109 overestimate discharge due to water back throw from Cahora Bassa.

Fig: 4.14 shows soil moisture simulated by the TOPMODEL for Manyame and Angwa sub catchments.



*Fig 4-14: Soil moisture simulated for Musengezi, Manyame & Angwa*

The distribution of soil moisture in the two catchments was close to rivers and was highly influenced by topography. The distribution of soil moisture was more distributed in the Angwa sub catchment than Manyame. For the surface layer; soil moisture changed corresponding to different slope positions. The areas furthest from the river channels showed the lowest moisture values. This is as a result of having two evaporating surfaces which are, being on the upland and slope. Inversely, the lower part of the side slope

showed the highest moisture values. This is as a result of having a higher supply of water from the other elevated areas in the catchment

The soil moisture maps demonstrate the impact of the presence of soil moisture on the surface energy dynamics in semi-arid areas and thus the high amount of soil moisture noted along the river channels. Specifically, soil moisture seems to be the most limited factor in the ecosystem restoration along the Mbire District (He et al., 1993). Overall the study showed that soil moisture was very low in the semi-arid Mbire District.

Figure 4-16 shows the variation for soil moisture in Chidodo which was measured by the Hobo data logger. This result was then compared with the volumetric soil moisture percentage in the same location as that of the simulated soil moisture. Taking mean soil moisture deficit ( $S_{bar}$ ) from 31 January a soil moisture map for Musengezi on that particular day was simulated.

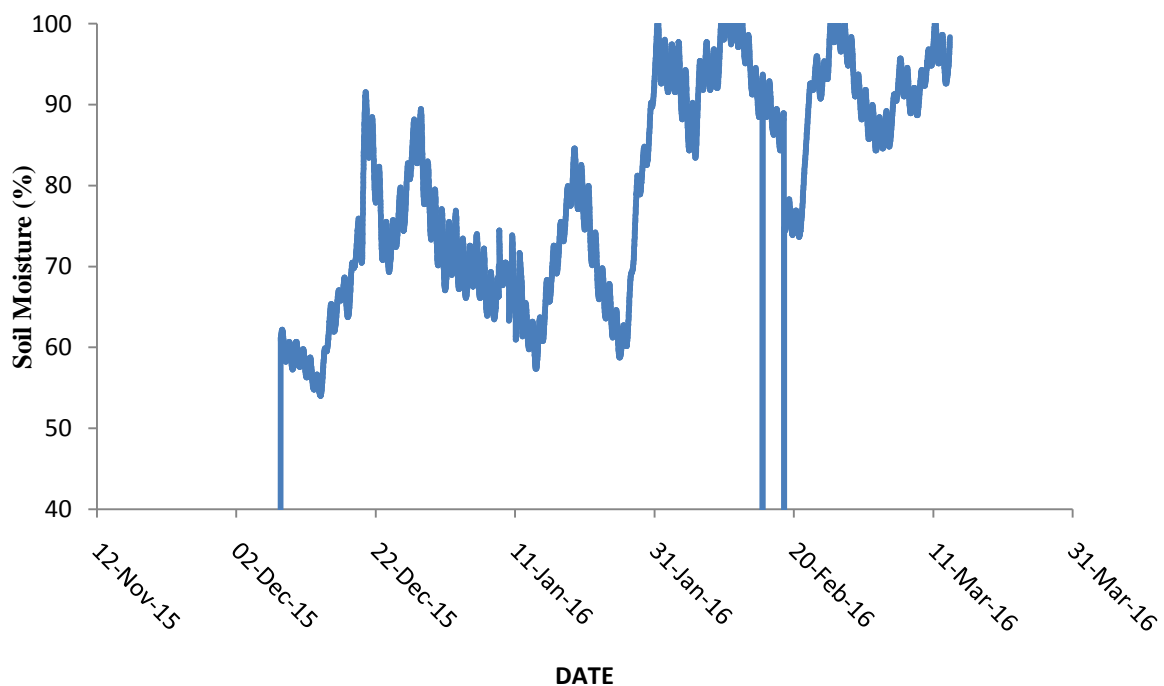


*Fig 4-15: Soil moisture from the data logger for Musengezi sub catchment*

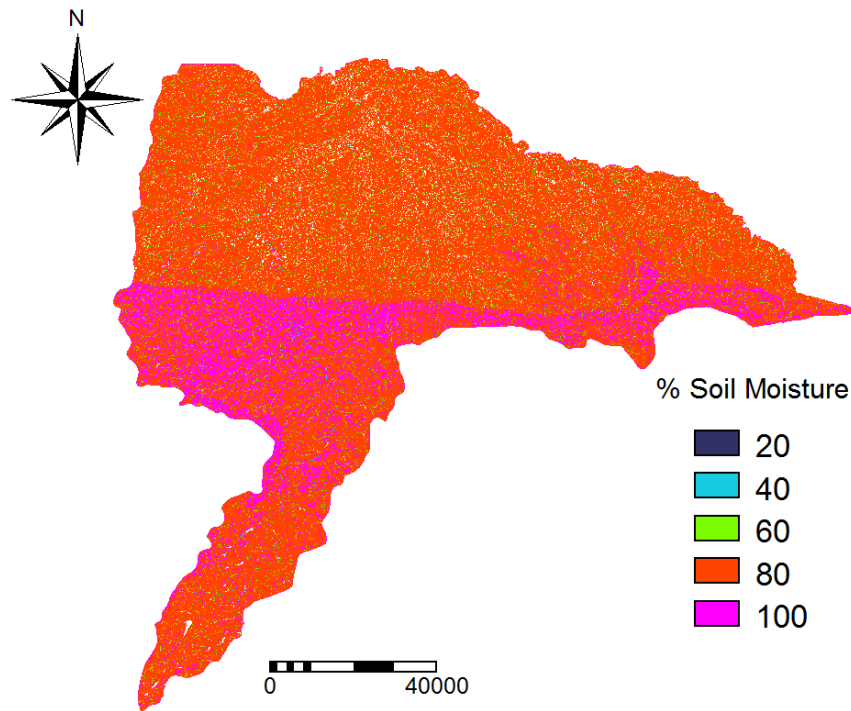


*Fig 4-16: Soil moisture simulated by TOPMODEL for Musengezi sub catchment*

The soil moisture on the 31<sup>st</sup> of January according to the Hobo data logger was 92 % of the maximum soil moisture. The soil moisture according to the simulated TOPMODEL was 80 %. The TOPMODEL simulation underestimated soil moisture by 12 % but it was a relatively good indicator as per the state of the soil moisture.

#### **4.4 Assessment of Water Availability in the Mbire District**

Two sets of data were used to conduct a water balance. The first used SEBS derived  $E_{TA}$  to determine closure. The second used TOPMODEL derived  $E_{TA}$  to determine the closure in the three sub catchments. A low value of closure (closest to 0 %) represents a good water balance for a catchment (reference). This means water in and out of the catchment is fully accounted for. After a water balance in the 3 sub catchments, Angwa sub catchment had the most efficient closure percentage of 7.4 % followed by Musengezi then Manyame. This may be due to the fact that the Angwa was the most efficiently gauged basin and has less effect of inflow from other basins than Manyame and Musengezi.

Table 4-6 shows the results for water balance with Actual Evapotranspiration being derived from SEBS.

Table 4-6: A water balance from 4/11/2015-31/01/2016 (SEBS  $E_{TA}$ )

Sub-basin	Precipitation (P)	Surface Inflow (Qin)m	Actual Evapotranspiration ( $E_{TA}$ )	Surface Outflow (Qout)	Closure (%)
Angwa	380	-	408	-	7.4
Manyame	402	133.7	420	204	16.5
Musengezi	394	-	429	15.51	12.8

Table 4-7 shows a water balance from 4/11/2015 to 31/01/2016 as estimated from the TOPMODEL  $E_{TA}$ . The water balance closure percentage for Angwa, Manyame and Musengezi are 11 %, 20 % and 16.1 % respectively. The result show a less effective closure when comparing with the closure derived from SEBS simulated  $E_{TA}$ .

In a study similar study in the Karkeh Basin of Iran, water closure values of between 0.6 % and 7.2 % in five out of the 7 sub-catchments which were analysed were presented (Muthuwatta et al., 2009). This was confirmation that partitioning a large catchment into smaller sub basins is an effective means of dealing with large un-gauged basins. In similar water balance which utilised remote sensing data to determine  $E_{TA}$  catchment similar to the Mbire District water balance (Deus et al., 2013).

Table 4-7: A water balance from 4/11/2015-31/01/2016 (TOPMODEL  $E_{TA}$ )

Sub-basin	Precipitation (P)	Surface Inflow (Qin)m	Actual Evapotranspiration ( $E_{TA}$ )	Surface Outflow (Qout)	Closure (%)
Angwa	380	-	421	-	11
Manyame	402	133.7	439	204	20.0
Musengezi	394	-	442	15.51	16.1

## 4.5 Conclusions

The following conclusions were drawn from the study:

1. Results from the regression analysis comparing methods of estimation of potential evapotranspiration against that of the FAO Penman Monteith method established

that the Penman and Makkink equations are the most accurate substitutes in this area. This was depicted by the high  $R^2$  values of 0.93 and 0.77 respectively.

2. There is an increasing trend of actual evapotranspiration using SEBS over the space of ten years in the month of October for the Mbire District. The largest values of  $E_{TA}$  are found in the densely forested areas (7 mm/day) as opposed to the minimum values found on the bare and grassed land (3.0 mm/day).
3. Low soil moisture values were simulated for Angwa sub-catchment compared to Manyame sub-catchment; this is mainly because of the high wetness index. The high soil moisture simulated by TOPMODEL was consistent with the soil moisture results measured from the data logger results. The TOPMODEL simulated results proved to be a good indicator of soil moisture as the percentage simulated was only 12 % below the data logger percentage soil moisture
4. Results from the water balance show satisfactory water balance closure of 7.2 % and 11 % in the Mbire district's Angwa basin for SEBS and TOPMODEL driven  $E_{TA}$  respectively. This proves that, determination of the water balance at sub basin scale rather than as the whole administrative boundary improves the ability to close the water balance.

#### **4.6 Recommendations**

1. Maintenance and replacement of gauging stations along the river channels, as well as increasing the number of weather stations is critical for optimal utilization of hydrological models and remote sensing techniques in Integrated Water Resource Management.
2. Future research on  $E_{TA}$  estimation using SEBS may consider taking readings twice a day (download two MODIS images) to decrease on generalization of mean daily  $E_{TA}$
3. Further research on water assessment maybe undertaken considering the northern side of the Zambezi River (Mozambique & Zambia) to decrease on biased approximations caused by varied administrative boundaries

## **References**

- Alexandris, S., Stricevic, R., Petkovic, S., 2008. Comparative analysis of reference evapotranspiration from the surface of rainfed grass in central Serbia, calculated six empirical methods against the Penman-Monteith formula. 17-28.
- Allen, R.G., Pereira, L.S., 1998. Crop evapotranspiration-Guidelines for computing crop water requirements, Rome, Italy.
- Anderson, M.C., Kustas, W.P., Alfieri, J.G., Gao, F., Hain, C., Prueger, J.H., Evett, S., Colaizzi, P., Howell, T., Chávez, J.L., 2012. Mapping daily evapotranspiration at Landsat spatial scales during the BEAREX'08 field campaign. *Advances in Water Resources* 50, 162–177.
- AWF, 2010. Mbire District Draft Natural Resources Management Plan, African Wildlife Foundation.
- Bandara, K.M.P.S., 2003. Monitoring irrigation performance in Sri Lanka with high-frequency satellite measurements during the dry season. *Agricultural Water Management* 58(2), 159-170.
- Bastiaanssen, W.G.M., Chandrapala, L., 2003. Water Balance Variability Across Sri Lanka for assessing agricultural and environmental water use. *Agricultural Water management* 58(2), 171-192.
- Bastiaanssen, W.G.M., Menenti, M., Feddes, R.A., Holtslag, A.A.M., 1998. A remote sensing surface energy balance algorithm for land (SEBAL). *Formulation. J. Hydrol*, 212–213, 198–212.
- Beck, M.B., 1991. Forecasting environmental change. *Journal of Forecasting* 10(1-2): 3-19. doi:10.1002/for.3980100103.
- Beljaars, A.C.M., Holtslag, A.A.M., 1991. Flux parameterization over land surfaces for atmospheric models. *J. Appl. Meteorol.* 30 (3), 327–341.
- Bergstrom, S., 1976. Development and application of a conceptual runoff model for Scandinavian catchments, SMHI Reports RHO, No. 7, Norrkoping.
- Bergstrom, S., 1992. The HBV model – its structure and applications, SMHI Reports RH, No. 4, Norrkoping.
- Beven, K., 1997. TOPMODEL: A CRITIQUE. *Hydrol. Process.* 11. 1069–1085.
- Beven, K., Freer, J., 2000. A dynamic TOPMODEL. *Hydrol. Process.* 15 (10), 1993–2011.

- Beven, K., Lamb, R., Quinn, P., Romanowicz, R., Freer, J., 1995. TOPMODEL. In: Sing.
- Beven, K.J., 1983. Surface water hydrology-runoff generation and basin structure. *Reviews of Geophysics* 21(3), 721-730.
- Beven, K.J., 2001. *Rainfall-Runoff Modelling The Primer*, John Wiley & Sons, Lancaster, UK.
- Beven, K.J., Kirkby, M.J., 1979. A physically based variable contributing area model of basin hydrology. *Hydrological Sciences-Bulletin-des Sciences Hydrologiques* 24(1), 43-69.
- Bloschl, G., Reszler, C., Komma, J., 2007. A spatially distributed flash flood forecasting model, *Environ. Modell. Software*, 23. 464–478.
- Brutsaert, W., 1982. *Evaporation into the Atmosphere: Theory, History, and Applications*. Reidel Publishing, Dordrecht.
- Brutsaert, W., 2005. *Hydrology: an introduction*. Cambridge University Press, Cambridge, p. 605.
- Brutsaert, W., Stricker, H., 1979. An advection-aridity approach to estimate actual regional evapotranspiration. *Water Resource* 443–450.
- Capehart, W.J., Carlson, T.N., 1997. Decoupling of surface and nearsurface soil water content: A remote sensing perspective. *Resour. Res.*, 33, 1383–1395.
- Chenje, M., 2000. *State of the environment Zambezi Basin 2000*. Maseru/Lusaka/Harare, SADC/IUCN/ZRA/SARDC.
- CIRAD, 2001. *The Mankind and the Animal in the Mid Zambezi Valley-Zimbabwe: Biodiversity Conservation and Sustainable Development in the Mid-Zambezi Valley.*, Librairie du Cirad, France.
- Crawford, N.H., Linsley, R.K., 1966. *Digital simulation in hydrology. Stanford Watershed Model IV*  
Department of Civil Engineering Stanford University, Stanford, California.
- De Fraiture, C., Cai, X., Rosegrant, M., Molden, D., Amarasinghe, U., 2003. Addressing the unanswered questions in global water policy: a methodology framework. *Irrig Drain*. 21–30.
- Dente, L., 2016. *Microwave Remote Sensing For Soil Moisture Monitoring: Synergy of Active And Passive Observations And Validation Of Retrieved Products*.

- Deus, D., Gloaguen, R., Krause, P., 2013. Water Balance Modeling in a Semi-Arid Environment with Limited in situ Data Using Remote Sensing in Lake Manyara, East African Rift, Tanzania.
- Dingman, S.L., 2002. Physical hydrology. Prentice Hall, Upper Saddle River.
- Duan, Z., Bastiaanssen, W.G.M., 2013. Estimating Water Volume Variations in lakes and reservoirs from four operational satellite altimetry databases and satellite imagery data. *Remote sensing environment* 134, 403-416.
- Dube, F., 2011. Spatial Erosion Hazard Assessment and Modelling in Mbire District, Zimbabwe: Implications for Catchment Management, Civil Engineering. University of Zimbabwe.
- Durand, P., Robson, A., Neal, C., 1992. Modeling the hydrology of sub-Mediterranean mountain catchments (Mont Loz'ere, France), using TOPMODEL: initial results. 139.1
- Eden, U., 2012. Drought Assessment By Evapotranspiration Mapping In Twente.
- FAO, 1996. Declaration of World Food Security. . World Food Summit. Rome, FAO.
- Federer, C.A., Vorosmarty, C.J., Fekete, B., 1996. Intercomparison of methods for calculating potential evaporation in regional and global water balance models. *Water Resources Research* 32 (7), 2315e2321.
- Garbrecht, J., Martz, L.W., 1999. Digital elevation model issues in water resources modeling. In: Proceedings from invited water resources sessions. ESRI international user conference.
- Garen, D.C., Moore, D.S., 2005. Curve number hydrology in water quality modeling: uses, abuses, and future directions. *Journal of the American Water Resources Association* 41(2), 377-388.
- Glenn, E.P., Huete, A.R., Nagle, P.L., Hirschboek, K.K., Brown, P., 2007. Intergrated Remote sensing and Ground Methods To Estimate Evapotranspiration. *Critical Reviews in Plant Science*, 139-168.
- Gonzales, A.S., Parodi, G., 2010. Estimation of actual evapotranspiration by Hydrus1D and its validation in REMEDHUS network, Spain. In: 1st International Congress of Hydrology in the Blue Plains, Buenos Aires, Argentina.
- Gowda, P.H., Chavez, J.L., Colaizzi, P.D., Evett, S.R., Howell, T.A., Tolk, J.A., 2008. ET mapping for agricultural water management: present status and challenges. *Irrigat*, 223–237.

- Gumindoga, W., 2010. Hydrologic Impacts of Landuse Change in the Upper Gilgel Abay River Basin, Ethiopia: TOPMODEL Application. University of Twente.
- Gumindoga, W., Rientjes, T.H.M., Haile, A.T., Dube, T., 2014. Predicting streamflow for land cover changes in the Upper Gilgel Abay River Basin, Ethiopia: A TOPMODEL based approach. *Physics and Chemistry of the Earth*, 3–15.
- Gumindoga, W., Rwasoka, D.T., Murwira, A., 2011. Simulation of streamflow using TOPMODEL in the Upper Save River catchment of Zimbabwe. *Physics and Chemistry of the Earth* 36, 806–813.
- Hassan, S.M.H., Amin, M.S.M., Shariff, A.R.M., 2003. Application of Remote Sensing and GIS for Rice Evapotranspiration Determination
- He, Y.C., Zhong, X.H., Zhang, N., Li, L.H., 1993. Basic laws of water and soil loss and the construction of protection forests in the Upper Reaches of the Changjiang River. In *Researches on the Chuanjiang Protection Forests in the Upper Reaches of the Changjiang River*, Yang YP. Science Press: Beijing; (in Chinese), 143–157.
- HEC, 2006. Hydrological Modelling (HEC-HMS) user`s Manual, in: Engineers, U.A.C.o. (Ed.).
- Hengl, T., Maathuis, B.H.P., Wang, L., 2007. Terrain parameterization in ILWIS. In: Hengl, Hannes, Reuter (Eds.), ‘Geomorphometry’ the Textbook. European Commission, DG Joint Research Centre, Institute for Environment and Sustainability, Land Management and Natural Hazards Unit, Ispra, Italy.
- Hobbins, M.T., Ramírez, J.A., Brown, T.C., Claessens, L.H.J.M., 2001. The complementary relationship in estimation of regional evapotranspiration: the complementary relationship areal evapotranspiration and advection-aridity models. *Water Resour. Res.* 37 (5), 1367–1387.
- Immerzeel, W.W., Droogers, P., Gieske, A.S.M., 2006. Remote sensing and evapotranspiration mapping: state of the art, FutureWater, Wageningen.
- ITC, 2007. ILWIS 3.31 Academic.
- Jia, L., Su, Z., Van den Hurk, B., Menenti, M., Moene, A., De Bruin, H.A.R., Yrisarry, J.J.B., Ibanez, M., Cuesta, A., 2003. Estimation of sensible heat flux using the Sensible Energy Balance System (SEBS) and ATSR measurements. *Physics and Chemistry Earth* 13, 75-88.

- Jia, L., Xi, G., Liu, S., Huang, C., Yan, Y., Liu, G., 2009. Regional estimation of daily to annual regional evapotranspiration with MODIS data in the Yellow River Delta wetland. *Hydrol. Earth Syst. Sci.* 13 (10), 1775–1787.
- Kirkby, M.J., Peel, R., Chisholm, R., Hagget, P., 1975. (a) TOPMODEL concept; flow direction calculation by (b) D8, (c) Dinf (Tarboton, 1997) algorithms., 69-90.
- Kusena, K., 2009. Landcover Change and Impact of Human-Elephant Conflict in The Zimbabwe, Mozambique and Zambia (ZiMoZa) Transboundary Natural Resources Area. CMB, Swedish Biodiversity Centre, Uppsala, Sweden.
- Kustas, W.P., Daughtry, C.S.T., 1990. Estimation of soil heat flux/net radiation ratio from spectral data. *Agric. Forest Meteorol* 49, 205–223.
- Leclerc, M.Y., Thurtell, G.W., 1990. Footprint prediction of scalar fluxes using a Markovian analysis. *Bound.-Layer Meteor.* 247–258.
- LGDA, 2009. Mbire District Baseline Survey Report, Lower Guruve Development Association.
- Liang, S., 2001. Narrowband to broadband conversions of land surface albedo I: algorithms. *Rem. Sens. Environ.* 76 (2), 213-238.
- Liou, Y.A., Kar, S., 2014. Evapotranspiration Estimation with Remote Sensing and Various Surface Energy Balance Algorithms.
- Liu, S., Bai, J., Jia, Z., Jia, L., Zhou, H., Lu, L., 2010. Estimation of evapotranspiration in the Mu Us Sandland of China. *Hydrol. Earth Syst. Sci.* 14 (3), 573–584.
- Maina, M.M., Amin<sup>1</sup>, M.S.M., Rowshon, M.K., Aimrun, W., Samsuzana, A.A., Yazid, M.A., 2014. Effects of crop evapotranspiration estimation techniques and weather parameters on rice crop water requirement. *AJCS* 8(4):495-501.
- Matinfar, H.R., 2012. Evapotranspiration estimation base upon SEBAL model and fieldwork
- Annals of Biological Research*, 2012, 3 (5), 2459-2463.
- McMahon, T.A., Pee, M.C., Lowe, L., Srikanthan, R., McVicar, T.R., 2013. Estimating actual, potential, reference crop and pan evaporation using standard meteorological data: a pragmatic synthesis. *Hydrol. Earth Syst. Sci.*, 17, 1331–1363.
- Moges, D.D., 2008. Land surface representation for regional rainfall-runoff modelling, upper Blue Nilebasin. Ethiopia.

- Moghadas, S., 2009. Long-term Water Balance of an Inland River Basin in an Arid Area, North-Western China.
- Molicova, H., Grimaldi, M., Bonell, M., Hubert, P., 1997. Using TOPMODEL towards identifying and modeling the hydrological patterns within a headwater, humid, tropical catchment. 11.9, 1169–1196.
- Monin, A.S., Obukhov, A.M., 1954. Osnovnye zakonomernosti turbulentnogo peremesivaniya v prizemnom sloe atmosfery (Basic laws of turbulent mixing in the ground layer of the atmosphere). Trudy Geofizicheskogo Inst. SSSR 24 (151), 163–187.
- Monteith, J.L., 1981. Evaporation and surface temperature. Quarterly Journal of the Royal Meteorological Society 107, 27.
- Muhammed, A.H., Enschede, 2012. Satellite based evapotranspiration estimation and runoff simulation: A TOPMODEL application to the Gilgel Abay catchment, Ethiopia. Geo-Information Science and Earth Observation. University of Twente.
- Muthuwatta, L.P., Booij, M.J., Rientjes, T.H.M., Bos, M.G., Gieske, A.S.M., Ahmad, M.U.D., 2009. Calibration of a semi-distributed hydrological model using discharge and remote sensing data.
- Nash, J.E., Sutcliffe, J.V., 1970. River flow forecasting through conceptual models. Part I: A discussion of principles. J. Hydrol. 10, 282–290.
- Norman, J.M., 2003. Remote sensing of surface energy fluxes at 10(1)-m pixel resolutions. Water Resources Research, 39(8).
- Nourani, V., Mano, A., 2007. Semi-distributed flood runoff model at the sub-continental scale for south-western Iran. 21.23, 3173–3180.
- NRCS, 2001. National Resources Conservation Service (NRCS), Section-4 Hydrology, in National Engineering Handbook. U.S. Department of Agriculture, Washington, D.C.
- Penkova, N.V., Shiklomanov, I.A., 2002. Water Balance Methodology for indirect assessment and prediction of basin water yield under human-induced land use changes Predictions in Ungauged Basins: PUB Kick-off.
- Phiri, M., 2011. An analysis of the Cahora Bassa dam water balance and reservoir operations and their flooding impact on upstream catchments, Civil Engineering. University of Zimbabwe, Harare.
- Pidwirny, M., 2006. Actual and Potential Evapotranspiration, Fundamentals of Physical Geography, 2nd Edition. .

- Ponce, V.M., 1989. *Engineering Hydrology, Principles and Practices*. Prentice Hall, New Jersey, USA.
- Ponce, V.M., Hawkins, R.H., 1996. Runoff curve number: has it reached maturity? *Journal of Hydrologic Engineering* 1(1), 11-19.
- Quinn, P.F., Beven, K.J., Chevallier, P., Planchon, O., 1991. The prediction of hill slope flow paths for distributed hydrological modeling using digital terrain models. 59–79.
- Rahman, H., Dedieu, G., 1994. SMAC: a simplified method for the atmospheric correction of satellite measurements in the solar spectrum. *Int. J. Rem. Sens.* 15 (1), 123–143.
- Ramírez, J.A., Hobbins, M.T., Brown, T.C., 2005. Observational evidence of the complementary relationship in regional evaporation lends strong support for Bouchet's hypothesis. *Geophys. Res. Lett.* 32 (15, L15401), 4.
- Robson, A.J., Whitehead, P.G., Johnson, R.C., 1993. An application of a physically based semi-distributed model to the Balquhidder catchments. 145(4), 357–370.
- Roerink, G.J., Su, Z., Menenti, M., 2000. S-SEBI: A simple remote sensing algorithm to estimate the surface energy balance. Part B: Hydrology, Oceans and Atmosphere 25(2), 147-157.
- Roy, D., Begam, S., Ghosh, S., Jana, S., 2013. CALIBRATION AND VALIDATION OF HEC-HMS MODEL FOR A RIVER BASIN IN EASTERN INDIA. *Journal of Engineering and Applied Sciences* 8.
- Rwasoka, D.T., Gumindoga, W., Gwenzi, J., 2011. Estimation of actual evapotranspiration using the Surface Energy Balance System (SEBS) algorithm in the Upper Manyame catchment in Zimbabwe. *J. Phys. Chem. Earth*, 1.
- Salama, M.A., Yousef, K.M., Mostafa A.Z., 2015. Simple equation for estimating actual evapotranspiration using heat units for wheat in arid regions. 8, 418–427.
- Santos, C.A.C., Bezerra, B.G., Silva, B.B., Rao, T.V.R., 2010. Assessment of daily actual evapotranspiration with SEBAL and S-SEBI algorithms in cotton crop. *Rev. bras. meteorol São Paulo* 25.
- Seibert, J., 1997. Estimation of Parameter Uncertainty in the HBV Model, *Nord. Hydrol.* 247–262.
- Shahidian. S., Serralheiro, R., Serrano, J., 2003. Hargreaves and Other Reduced-Set Methods for Calculating Evapotranspiration
- Sobrino, J.A., Kharraz, J.E., Li, Z.L., 2003. Surface temperature and water vapour retrieval from MODIS data. . *Int. J. Rem. Sens.* 24 (24), 5161–5182.

- Sobrino, J.A., Raissouni, N., 2000. Toward remote sensing methods for land cover dynamic monitoring. Application to Morocco. *Int. J. Rem. Sens.* 21 (2), 353–366.
- Srinivasan, K., Poongothai, S., 2013. WATER BALANCE OF WELLINGTON TANK IRRIGATED WATERSHED USING SCS CURVE NUMBER AND GIS. *International Journal of Civil Engineering (IJCE)*.
- Su, Z., 2002. The Surface Energy Balance System (SEBS) for estimation of turbulent heat fluxes. *Hydrology. Earth Syst. Sc.* 6, 85-99.
- Sugita, M., Brutsaert, W., 1991. Daily evaporation over a region from lower boundary layer profiles measured with radiosondes.
- Takeuchi, K., Hapuarachchi, P., Zhou, M., Ishidaira, H., Magome, J., 2008. A BTOP model to extend TOPMODEL for distributed hydrological simulation of larg basins. *Hydrol. Process.* 22.17, 3236–3251.
- Troch, P.A., 2000. Data Assimilation for Regional Water Balance Studies in Arid and Semi-arid Areas (Case Study: The Volta Basin Upstream the Akosombo Dam in Ghana). . In *Proceedings of the First MSG RAO Workshop, European Space Agency ESASP-452, Bologna, Italy*, 163.
- Ukkola, A.M., Prentice, I.C., 2013. A worldwide analysis of trends in water-balance evapotranspiration. *Hydrol. Earth Syst. Sci.* 4177–4187.
- van den Hurk, B.J.J.M., Holtslag, A.A.M., 1997. On the bulk parameterization of surface fluxes for various conditions and parameter ranges. . *Boundary-Lay. Meteorol.* 82 (1), 119–133.
- Wieringa, J., 1986. Roughness-dependent geographical interpolation of the surface wind speed averages. *Quart. J. Roy. Meteor. Soc.* 867–889.
- Woodward, D.E., Hawkins, R.H., Quan, Q.D., 2002. Curve number method: origins, applications and limitations., In: *Hydrologic Modeling for the 21st Century, Second Federal Interagency Hydrologic Modeling Conference, Las Vegas, Nevada*.
- Worlock, M.D., 1995. Effects of sub basin size on topographic charecteristic and simulated flow paths in Sleepers River Watershed, Vermont. 31.8.
- Xiong, L., Guo, S., 2004. Effects of the catchment coefficient on the performance of TOPMODEL in rainfall-runoff modelling. *Hydrol. Process* 18.10, 1823–1836

- Yang, L., Wei, W., Chen, L., Jia, F., Mo, B., 2012. Spatial variations of shallow and deep soil moisture in the semi-arid Loess Plateau, China. *Hydrol. Earth Syst. Sci.*
- Yanmin, Y., Yonghui, Y., De, L.L., Tom, N., Bingfang, W., Nana, Y., 2014. Regional Water Balance Based on Remotely Sensed Evapotranspiration and Irrigation: An Assessment of the Haihe Plain, China. 2514-2533.
- Yu, Z., Carlson, T.N., Barron, E.J., Schwartz, F.W., 2001a. On evaluating the spatial-temporal variation of soil moisture the Susquehanna River Basin. *WATER RESOURCES RESEARCH* 37, 1313–1326.
- Yu, Z.B., White, R.A., Guo, Y.J., Voortman, J., Kolb, P.J., Miller, D.A., Miller, A., 2001b. Stormflow simulation using a geographical information system with a distributed approach. *Journal of the American Water Resources Association* 37(44), 957-971.
- ZIMASSET, 2013. Zimbabwe agenda for sustainable socio economic transformation.
- ZimStat, 2012. Zimbabwe Census 2012 : Preliminary Report. Harare, Zimbabwe National Statistics Agency.

## **APPENDICES**

### **Appendix 1: SEBS SCRIPT RUN in ILWIS 3.4 or 3.7**

```
!gdal_translate.exe '-of' ILWIS 'C:\SEBS\Julian_305_mbire\_ev_1km_emissive_b10.tif'  
'C:\SEBS\Julian_305_mbire\band31_dn' //THIS IS THE IMPORTING STAGE  
!gdal_translate.exe '-of' ILWIS 'C:\SEBS\Julian_305_mbire\_ev_1km_emissive_b11.tif'  
'CD:\SEBS\Julian_305_mbire\band32_dn'  
!gdal_translate.exe '-of' ILWIS 'C:\SEBS\Julian_305_mbire\_ev_1km_refsb_b11.tif'  
'C:\SEBS\Julian_305_mbire\band17_dn'  
!gdal_translate.exe '-of' ILWIS 'C:\SEBS\Julian_305_mbire\_ev_1km_refsb_b12.tif'  
'C:\SEBS\Julian_305_mbire\band18_dn'  
!gdal_translate.exe '-of' ILWIS 'C:\SEBS\Julian_305_mbire\_ev_1km_refsb_b13.tif'  
'C:\SEBS\Julian_305_mbire\band19_dn'  
!gdal_translate.exe '-of' ILWIS  
'C:\SEBS\Julian_305_mbire\_ev_250_aggr1km_refsb_b0.tif'  
C:\SEBS\Julian_305_mbire\band1_dn'  
!gdal_translate.exe '-of' ILWIS  
'C:\SEBS\Julian_305_mbire\_ev_250_aggr1km_refsb_b1.tif'  
'C:\SEBS\Julian_305_mbire\band2_dn'  
!gdal_translate.exe '-of' ILWIS  
'C:\SEBS\Julian_305_mbire\_ev_500_aggr1km_refsb_b0.tif'  
'C:\SEBS\Julian_305_mbire\band3_dn'  
!gdal_translate.exe '-of' ILWIS  
'C:\SEBS\Julian_305_mbire\_ev_500_aggr1km_refsb_b1.tif'  
'C:\SEBS\Julian_305_mbire\band4_dn'  
!gdal_translate.exe '-of' ILWIS  
'C:\SEBS\Julian_305_mbire\_ev_500_aggr1km_refsb_b2.tif'  
'C:\SEBS\Julian_305_mbire\band5_dn'  
!gdal_translate.exe '-of' ILWIS  
'C:\SEBS\Julian_305_mbire\_ev_500_aggr1km_refsb_b3.tif'  
'C:\SEBS\Julian_305_mbire\band6_dn'
```

```
!gdal_translate.exe '-of' ILWIS
'C:\SEBS\Julian_305_mbire\_ev_500_aggr1km_refsb_b4.tif'
'C:\SEBS\Julian_305_mbire\band7_dn'
!gdal_translate.exe '-of' ILWIS 'C:\SEBS\Julian_305_mbire\_height.tif'
'D:\SEBS\Julian_305_mbire\height'
!gdal_translate.exe '-of' ILWIS 'C:\SEBS\Julian_305_mbire\_sensorzenith.tif'
'C:\SEBS\Julian_305_mbire\vza_dn'
!gdal_translate.exe '-of' ILWIS 'C:\SEBS\Julian_305_mbire\_solarazimuth.tif'
'C:\SEBS\Julian_305_mbire\saa_dn'
!gdal_translate.exe '-of' ILWIS 'C:\SEBS\Julian_305_mbire\_solarzenith.tif'
'C:\SEBS\Julian_305_mbire\sza_dn' !gdal_translate.exe '-of' ILWIS
'C:\SEBS\Julian_305_mbire\_sensorazimuth.tif' 'C:\SEBS\APRIL_15\vaa_dn'
//At this stage we are converting to radiances and reflectances getting the data from HDF
Viewer
band1.mpr = MapSI2Radiance(band1_dn,0.0000525993,-0)
band2.mpr = MapSI2Radiance(band2_dn,0.0000317887,-0)
band3.mpr = MapSI2Radiance(band3_dn,0.0000525202,-0)
band4.mpr = MapSI2Radiance(band4_dn,0.0000424674,-0)
band5.mpr = MapSI2Radiance(band5_dn,0.0000399907,0)
band6.mpr = MapSI2Radiance(band6_dn,0.0000354509,0)
band7.mpr = MapSI2Radiance(band7_dn,0.0000290592,0)
band31.mpr = MapSI2Radiance(band31_dn,0.0008400220,1577.33970)
band32.mpr = MapSI2Radiance(band32_dn,0.0007296976,1658.22130)
sza = sza_dn * 0.01
saa = saa_dn * 0.01
vza = vza_dn * 0.01
vaa = vaa_dn * 0.01
btm31.mpr = MapBrightnessTemperature(MODIS,band31,band32,btm32)//Brightness
temperature calculation
band1_smac.mpr =
MapSMAC(band1,C:\SEBS\Julian_305_mbire\coefficients\coef_MODIS1_CONT.dat,0,0.3
00000,1,C:\SEBS\Julian_305_mbire\watervapour.mpr,0,0.288000,0,768,1,C:\SEBS\Julian
```

*\_305\_mbire\sza.mpr, I, C:\SEBS\Julian\_305\_mbire\saa.mpr, I, C:\SEBS\Julian\_305\_mbire\  
vza.mpr, I, C:\SEBS\Julian\_305\_mbire\vaa.mpr)*

*band2\_smac.mpr =*

*MapSMAC(band2, C:\SEBS\Julian\_305\_mbire\coefficients\coef\_MODIS2\_CONT.dat, 0, 0.3  
00000, I, C:\SEBS\Julian\_305\_mbire\watervapour.mpr, 0, 0.288, 0, 768, I, C:\SEBS\Julian\_30  
5\_mbire\sza.mpr, I, C:\SEBS\Julian\_305\_mbire\saa.mpr, I, C:\SEBS\Julian\_305\_mbire\vza.  
mpr, I, C:\SEBS\Julian\_305\_mbire\vaa.mpr)*

*band3\_smac.mpr =*

*MapSMAC(band3, C:\SEBS\Julian\_305\_mbire\coefficients\coef\_MODIS3\_CONT.dat, 0, 0.3  
, I, C:\SEBS\Julian\_305\_mbire\watervapour.mpr, 0, 0.288, 0, 768, I, C:\SEBS\Julian\_305\_mbi  
re\sza.mpr, I, C:\SEBS\Julian\_305\_mbire\saa.mpr, I, C:\SEBS\Julian\_305\_mbire\vza.mpr, I,  
C:\SEBS\Julian\_305\_mbire\vaa.mpr)*

*band4\_smac.mpr =*

*MapSMAC(band4, C:\SEBS\Julian\_305\_mbire\coefficients\coef\_MODIS4\_CONT.dat, 0, 0.3  
, I, C:\SEBS\Julian\_305\_mbire\watervapour.mpr, 0, 0.288, 0, 768, I, C:\SEBS\Julian\_305\_mbi  
re\sza.mpr, I, C:\SEBS\Julian\_305\_mbire\saa.mpr, I, C:\SEBS\Julian\_305\_mbire\vza.mpr, I,  
C:\SEBS\Julian\_305\_mbire\vaa.mpr)*

*band5\_smac.mpr =*

*MapSMAC(band5, C:\SEBS\Julian\_305\_mbire\coefficients\coef\_MODIS5\_CONT.dat, 0, 0.3  
00000, I, C:\SEBS\Julian\_305\_mbire\watervapour.mpr, 0, 0.288, 0, 768, I, C:\SEBS\Julian\_30  
5\_mbire\sza.mpr, I, C:\SEBS\Julian\_305\_mbire\saa.mpr, I, C:\SEBS\Julian\_305\_mbire\vza.  
mpr, I, C:\SEBS\Julian\_305\_mbire\vaa.mpr)*

*band7\_smac.mpr =*

*MapSMAC(band7, C:\SEBS\Julian\_305\_mbire\coefficients\coef\_MODIS7\_CONT.dat, 0, 0.3  
, I, C:\SEBS\Julian\_305\_mbire\watervapour.mpr, 0, 0.288, 0, 768, I, C:\SEBS\Julian\_305\_mbi  
re\sza.mpr, I, C:\SEBS\Julian\_305\_mbire\saa.mpr, I, C:\SEBS\Julian\_305\_mbire\vza.mpr, I,  
C:\SEBS\Julian\_305\_mbire\vaa.mpr)*

*albedo.mpr =*

*MapAlbedo(C:\SEBS\Julian\_305\_mbire\band1\_smac.mpr, D:\SEBS\APRIL\_15\band2\_sm  
ac.mpr, modis, band3\_smac, band4\_smac, band5\_smac, band7\_smac)//Land surface albedo  
computation*

*emis.mpr =*

*MapEmissivity(band1\_smac, band2\_smac, albedo, MODIS, ndvi, emis\_dif, nomap)// this*

*stage produces more than one map ,Land surface emissivity, NDVI, vegetation proportion and emissivity difference computation*

*lst.mpr =*

*MapLandSurfaceTemperature(MODIS,btm31,btm32,emis,emis\_dif,watervapour)//This is the stage where Land surface temperature computation*

*sebs\_evapo.mpr =*

*MapSEBS(lst,emis,albedo,ndvi,0,0,,1,sza,0,1,height,0,1,105,0,0,0,2,1000,0,,0.006,0,,6,0,,2*

*0,0,,100000,0,,100100,39.2,1,1025,0,nomap,0,nomap,0,nomap,0,nomap,0,,20,0,,10,1,2.5,,*

*0)//This is the combination of all the inputs we have been creating SEBS Relative Evapotranspiration for Mbire District*

## **Appendix 2: SOIL MOISTURE SETUP IN THE MUSENGEZI SUB-CATCHMENT**



### **Appendix 3: AUTOMATED WEATHER STATION SETUP AT CHIDODO CLINIC**

